A THERMO-CHEMICAL ANALYSIS OF SOME AMPHIBOLES

by

MARK   CAESAR   WITTELS

B.S., University of Minnesota

(1947)

SUBMITTED IN PARTIAL FULFILLMENT OF THE

REQUIREMENTS FOR THE DEGREE OF

DOCTOR OF PHILOSOPHY

at the

MASSACHUSETTS INSTITUTE OF TECHNOLOGY

(1951)

Signature of Author. . . . .
                            Department of Geology, Feb. 16, 1951

Certified by . . . .
                                              Thesis Supervisor

. . . .
    Chairman, Departmental Committee on Graduate Students

TABLE OF CONTENTS

PART I

MINERAL CALORIMETRY

ABSTRACT

A THERMO-CHEMICAL ANALYSIS OF SOME AMPHIBOLES

By Mark Caesar Wittels

Submitted for the degree of Doctor of Philosophy in the Department of Geology on February 16, 1951.

It is well known that at temperatures above $600°C$. the amphiboles undergo characteristic physical and chemical changes. In this investigation, a new quantitative technique of analysis was established for measuring the energy changes.

To do this a differential thermal analyzer was calibrated to measure energy changes as small as 0.1 calories in the temperature range $600°C.-1125°C$. Spectrochemical and x-ray powder diffraction methods were employed in conjunction with the thermal techniques.

A selected suite of orthorhombic and monoclinic amphiboles was analyzed for (1) the thermal nature of the $(OH,F)_2$ group, (2) oxidation of ferrous iron above $700°C.$,(3) structural disintegration characteristics, (4) structural transformations below temperatures of dissociation, and (5) minor elements.

Weight-loss determinations for H_2O and spectrochemical analyses for F gave experimental results which closely approached the theoretical values for (H_2O+F). It was shown that many low chemical determinations for this group may be due to inaccurate analyses for H_2O and the absence of spectrochemical analyses for F. Low H_2O analyses cannot be attributed to the oxidation of Fe^{++} during dehydration experiments because samples containing less than 15% FeO need no extra-structural oxygen for the reaction. Fluorine was not driven off at $1125°C$. and it remained in the reaction products of structural disintegration, usually as an alkali-fluoride glass. The presence of fluorine was observed to speed the reaction velocity of structural collapse.

The oxidation of ferrous iron in amphiboles was measured calorimetrically by differential thermal analysis. The experimental determinations for the heat of reaction were 2-5 times less than the theoretical determinations. It was concluded that the extreme sluggishness of the reaction diminished the sensitivity of the thermographic response.

The anthophyllites transform monotropically into ortho-pyroxene, cristobalite, glass, and water near $1000°C$. Calorimetric determinations for 3 magnesian species gave heats of reaction ($+\Delta H$) between 1.50 and 4.50 calories per gram. In 4 ferrous specimens the heats of reaction varied between 0.33 and 2.66 calories per gram. The formation of a glass in the reaction products of the ferrous varieties triggered the reaction so that smaller amounts of heat were absorbed by the disintegration.

Above $925°C$. the monoclinic amphiboles transform in the solid state into the following products:(monoclinic pyroxene),(cristobalite),(plagioclase),(hematite), (olivine),(magnetite),(water),and (glass). The heats of reaction ($+\Delta H$) for tremolite, richterite, and glaucophane end-members were near 6.50 calories per gram. Hastingsite varieties disintegrate with a smaller absorption of heat (avg. = 2.33 cal. per gram).

Mg anthophyllite contracts in the c-axis direction at $830°C$. The linear contraction is 0.44% and 2.75 cal.per gm. are evolved. The shrinkage is reversible if $830°C$. is not exceeded, and no displacive transformation was detected. The reaction could not be reversed thermographically.

At $825°C$. tremolite undergoes an irreversible c-axis contraction of 0.65%. The heat evolved in the transformation is approximately 2.75 calories per gram.

An irreversible crystallographic contraction in a richterite specimen was observed at $825°C$. X-ray methods revealed axial contractions of 0.33% a_0, 0.44% b_0, and 0.55% c_0. The average coefficient of linear thermal contraction is 2.8×10^{-5} per degree C. as an approximate determination.

Minor element analyses for 7 anthophyllites indicated a major division between Mg and Fe varieties. The analysis of the monoclinic amphiboles was not so noteworthy. The high concentration of Ni and Cr was dominant in metamorphic magnesium-rich amphiboles.

ABSTRACT

It is well known that at temperatures above 600°C. the amphiboles undergo characteristic physical and chemical changes. In this investigation, a new quantitative technique of analysis was established for measuring the energy changes.

To do this a differential thermal analyzer was calibrated to measure energy changes as small as 0.1 calories in the temperature range 600°C.-1125°C. Spectrochemical and x-ray powder diffraction methods were employed in conjunction with the thermal techniques.

A selected suite of orthorhombic and monoclinic amphiboles was analyzed for:

(1) The thermal nature of the $(OH,F)_2$ group.

(2) Oxidation of ferrous iron above 700°C.

(3) Structural disintegration characteristics.

(4) Structural transformations below temperatures of dissociation.

(5) Minor elements.

Weight-loss determinations for H_2O and spectro-chemical analyses for F gave experimental results which closely approached the theoretical values for (H_2O+F). It was shown that many low chemical determinations for this

group may be due to inaccurate chemical analyses for H_2O and the absence of spectrochemical analyses for F. Low H_2O analyses cannot be attributed to the oxidation of Fe^{++} during dehydration experiments because samples containing less than 15% FeO need no extra-structural oxygen for the reaction. Fluorine was not driven off at $1125°C$. and it remained in the reaction products of structural disintegration, usually as an alkali-fluoride glass. The presence of fluorine was observed to speed the reaction velocity of structural collapse.

The oxidation of ferrous iron in amphiboles was measured calorimetrically by differential thermal analysis. The experimental determinations for the heat of reaction were two to five times less than the theoretical determinations in most specimens. It was concluded that the extreme sluggishness of the reaction diminished the sensitivity of the thermographic response.

The anthophyllites transform monotropically into ortho-pyroxene, cristobalite, glass, and water near $1000°C$. Calorimetric determinations for three magnesian varieties gave heats of reaction $(+\Delta H)$ between 1.50 and 4.50 calories per gram. In four ferrous specimens the heats of reaction varied between 0.33 and 2.66 calories per gram. The formation of a glass in the reaction products of the ferrous varieties triggered the reaction so that smaller amounts of heat were absorbed by the disintegration.

Between 925°C. and 1125°C. the monoclinic amphiboles transform monotropically into simpler structural units that are stable at these elevated temperatures. The transformation occurs in the solid state with the following substances among the disintegration products: (1) monoclinic pyroxene, (2) cristobalite, (3) plagioclase, (4) hematite, (5) olivine, (6) magnetite, (7) water, and (8) glass. The heats of reaction ($+\Delta H$) for tremolite, actinolite, richterite, and glaucophane end-members were near 6.50 calories per gram. Pargasite-hastingsite end-members disintegrate at 1080°C. with a smaller absorption of heat. In three samples the average amount of heat absorbed was 2.33 calories per gram.

Magnesian anthophyllite undergoes a volume contraction in the c-axis direction at about 830°C. The transformation is reversible if this temperature is not exceeded, and the change determined was a linear contraction of approximately 0.44%. Quenched specimens revealed no displacive transformation and the reaction could not be reversed thermographically. A reaction evolving 2.75 calories per gram was measured.

Tremolite undergoes a volume contraction in the c-axis direction at about 825°C. A linear shrinkage of 0.65% was observed but the transformation was not reversible thermographically or dilatometrically. The heat evolved in

the transformation is approximately 2.75 calories per gram.

A specimen of richterite quenched from 825°C. and examined by x-ray methods revealed a crystallographic contraction at that temperature. The approximate axial contractions are 0.33% a_o, 0.44% b_o, and 0.55% c_o, and the transformation is irreversible. A calculation for the average coefficient of linear thermal contraction gave a value of 2.8×10^{-5} per degree C.

Minor element determinations for seven anthophyllites indicated a major division between magnesian and ferrous varieties. The analysis of sixteen monoclinic amphiboles was not nearly so noteworthy. The outstanding feature of the entire minor element determination was the high concentration of Ni and Cr in the metamorphic magnesium-rich varieties.

Introduction

The technique of differential thermal analysis has been largely confined to the investigation of the qualitative thermal characteristics of various mineral species. A large number of minerals have been studied by this method, particularly the clay minerals.

The ceramists[1],[2],[3] have developed semi-quantitative techniques for the determination of the per cent mineral constituents in various ceramic bodies, using the alpha-beta quartz inversion as the standard reference in the differential thermal curve. These methods have not been of a truly calorimetric nature, but they have shown the way for the subsequent advances of the use of the differential thermal analyzer as a calorimetric tool.

Cohn[4], Macgee[5], and Shorter[6] have described calibrations of differential thermal analyzers for use on ceramic bodies which advanced the use of the instrument to a more quantitative basis, although still on a comparatively macro scale.

Described here is the calibration of a differential thermal analyzer to detect and also to measure heat changes as small as 0.010 calories in magnitude.

Apparatus

The apparatus used in this investigation was essentially the same as that described by Whitehead and Breger[7]. The controller and recorder were unchanged but the mass of the entire furnace housing was reduced so that the relation of sample block and furnace wall is that shown in Fig. 1. As a result of these changes the furnace was brought under closer temperature control, especially at high heating rates, and thermal changes as recorded by the thermographic curves became highly magnified.

Calibration

Theoretical Basis:

Briefly reviewed, here is the theoretical basis for quantitative measurements with the differential thermal analyzer as formulated by Speil[3], using Fig. 2 as a sample thermographic curve showing a reaction beginning at point a and continuing towards point c.

$$(\text{Area}) \ abc \propto \int_a^c \Delta T \ dt = \frac{M(\Delta H)}{gk} \tag{1}$$

where,

M = mass of the reacting specimen

ΔH = specific heat of reaction

g = geometrical shape constant

and k = thermal conductivity of the reacting specimen
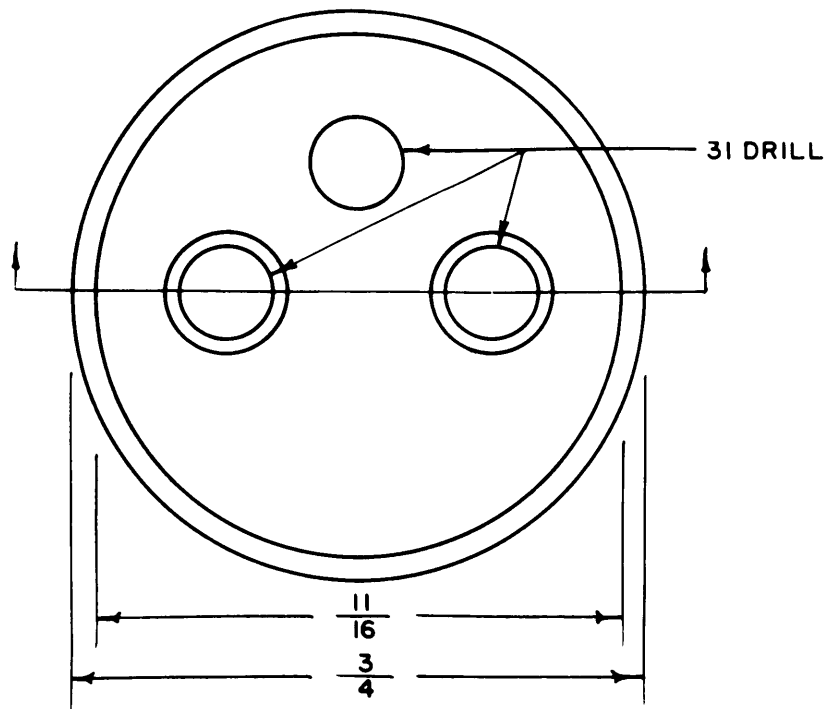
FIG. 1
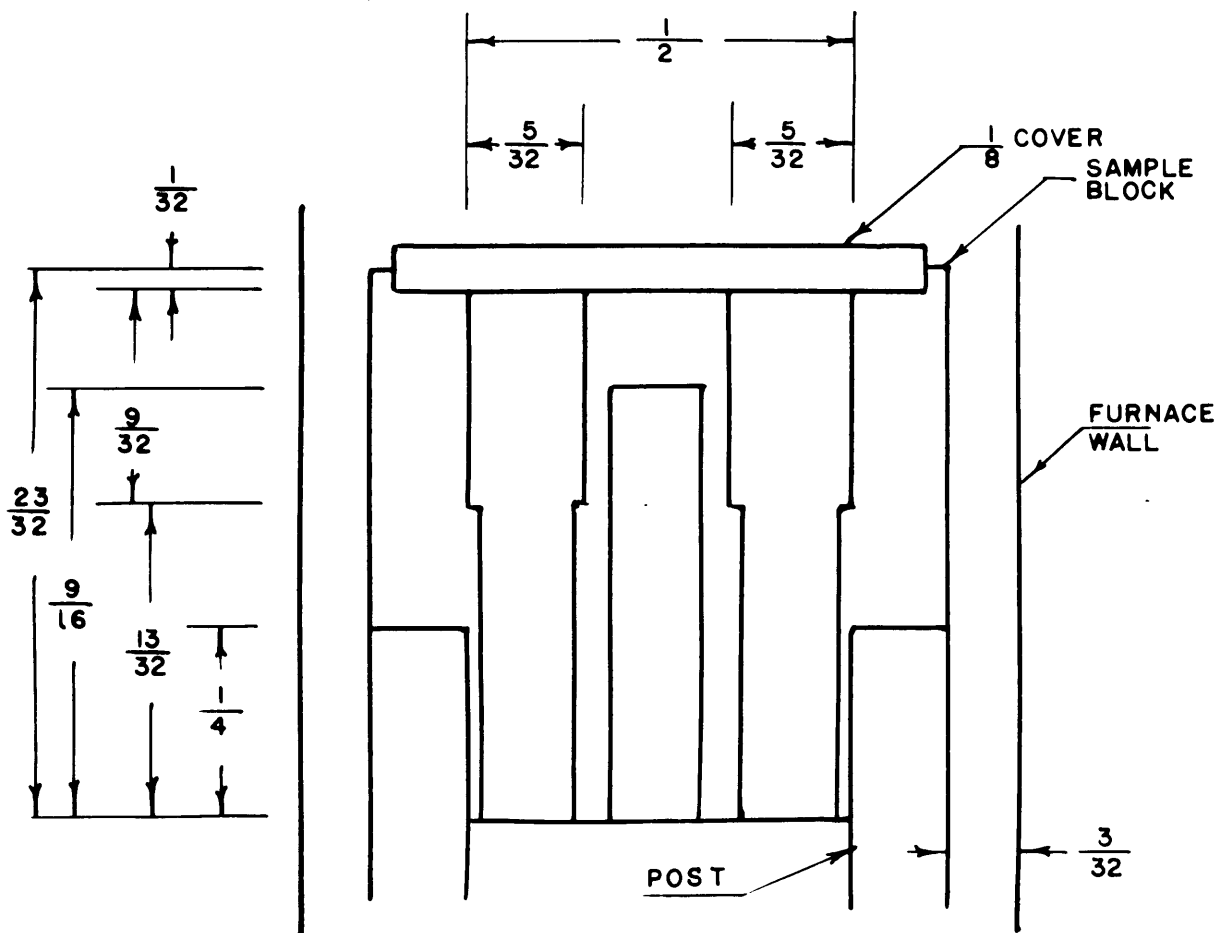
FIG. 2
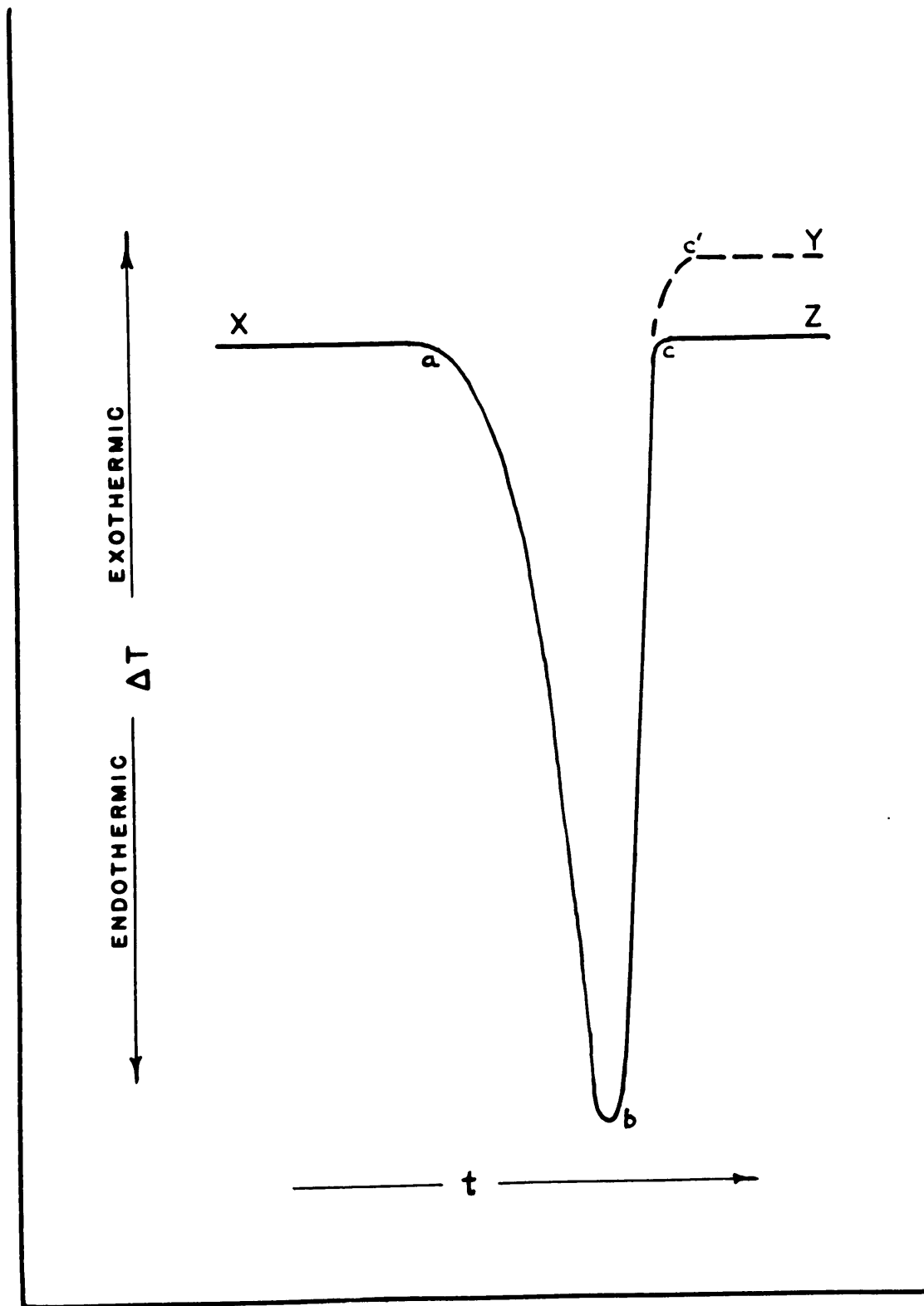
Equation (1) neglects the temperature gradient in the sample as well as some insignificant differential terms, and therefore is a close approximation. Transposing terms we get,

$$\text{(Area) } abc \propto gk \int_a^c \Delta T dt = M \Delta H = Q \qquad (2)$$

or, $\qquad$ (Area) $abc \propto Q \qquad\qquad$ (3)

As an approximation, then, the area is a linear function of the heat of reaction as expressed by Equation (3). Later, the restriction imposed on the validity of this equation by the above-mentioned neglect of temperature gradient in the sample will be shown.

Method:

Briefly, the method of calibration involved heating carefully weighed samples of a known reactive substance at a constant rate through its reaction temperature range and then relating the energy changes with the corresponding thermographic responses (areas) recorded by the curves. The inert standard in all these experiments was δ Al_2O_3.

The reactive substance chosen for the calibration was $CaCO_3$ (calcite) which follows the reaction

$$CaCO_3 + Q = CaO + CO_2$$
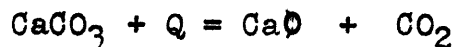
beginning at a temperature of about $630°C$. when heated statically.

The values for $Q^{(7A)}$ in the above reaction are very
large and permitted samples as small and smaller than the
thermocouple head to be used. Single cleavage rhombs were
chosen because of ease of handling. Equation (3) was shown
to be valid in these experiments because the minute size of
the samples eliminated the possibility of temperature gradient
effects, which are to be expected in samples of greater volume.

The dissociation of the $CaCO_3$ samples was thermo-
graphically recorded at heating rates of 10°C., 15°C., 22.5°C.,
and 30°C., per minute in the evacuated furnace. The relation
between the thermographic responses (areas) and the heats of
reaction, as described by Equation (3) are shown in Fig. 3.
The validity of Equation (3) is established by the linear
relations shown. Table I is a summation of the experimental
and calculated data for this calibration, and Figures 4 and 5
show the thermographic responses.

Measurement of areas was made with a planimeter and
checked by means of a simple grid. This measurement was the
crux of the entire calibration since the area is not always
clearly defined. In Fig. 2, the thermographic base-line X-Z
is not linear in the general case. It is obvious that when
a large sample is tested in the analyzer a major reaction is
usually accompanied by a sharp change in the thermal conduc-
tivity and the specific heat capacity of the specimen. This
results in a thermal gradient between the differential
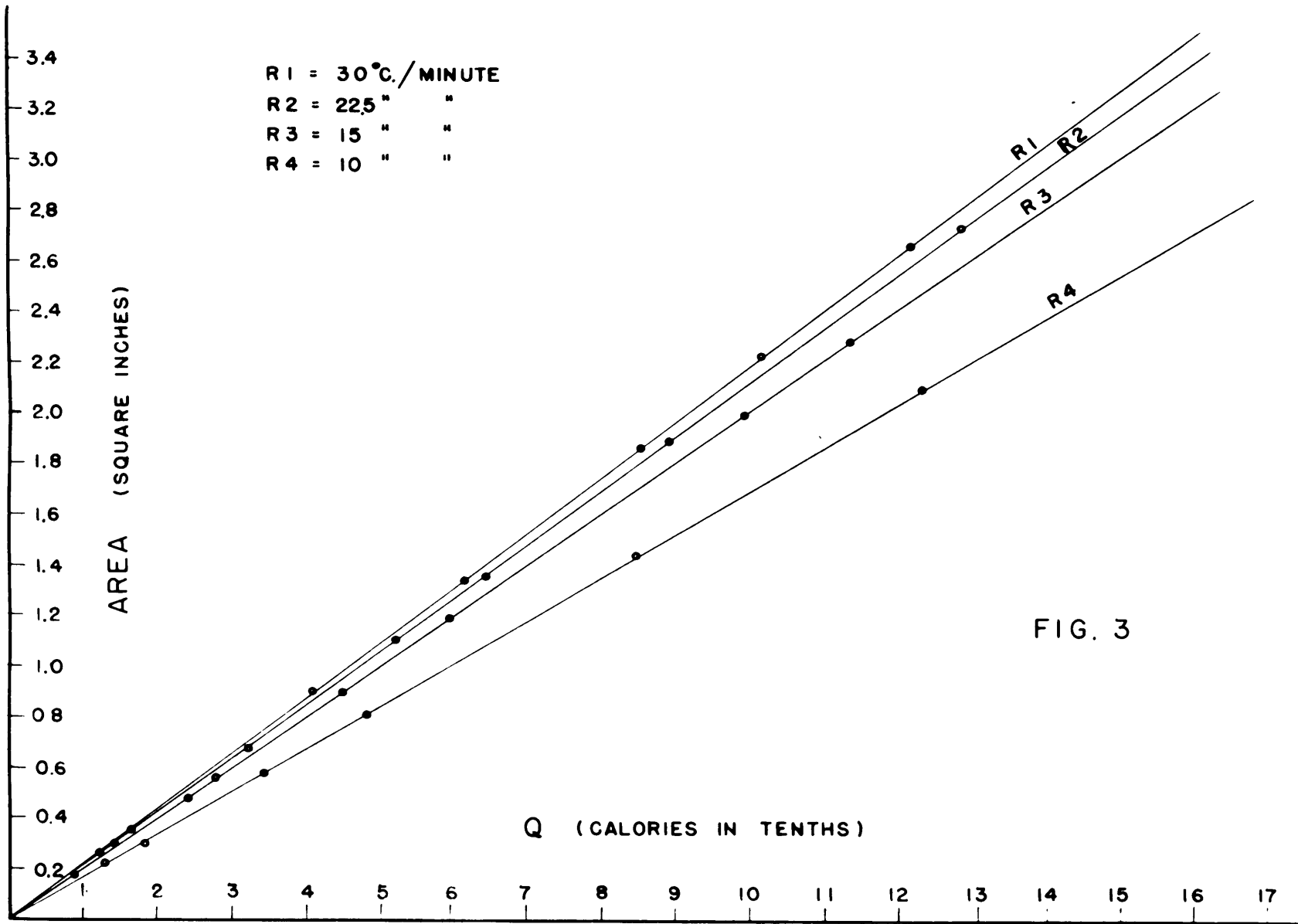
FIG. 3

TABLE I

Sample Designation		Weight (milligm)	Heat of Reaction (tenths of calories)	Thermographic Response (Area in sq.in.)
R1	A	0.30	1.23	0.29
	B	0.40	1.65	0.36
	C	1.00	4.10	0.90
	D	1.50	6.14	1.39
	E	2.10	8.53	1.91
	F	2.50	10.15	2.28
	G	3.00	12.15	2.72
R2	U	0.40	1.68	0.36
	V	0.80	3.27	0.70
	W	1.30	5.27	1.12
	X	1.60	6.51	1.39
	Y	2.20	8.93	1.95
	Z	3.15	12.76	2.78
R3	N	0.20	0.82	0.18
	O	0.60	2.43	0.48
	P	0.70	2.83	0.56
	Q	1.10	4.47	0.90
	R	1.45	5.88	1.22
	S	2.45	9.92	2.04
	T	2.80	11.39	2.34
R4	H	0.30	1.22	0.22
	I	0.45	1.82	0.33
	J	0.85	3.44	0.60
	K	1.20	4.85	0.86
	L	2.10	8.50	1.48
	M	3.05	12.24	2.18
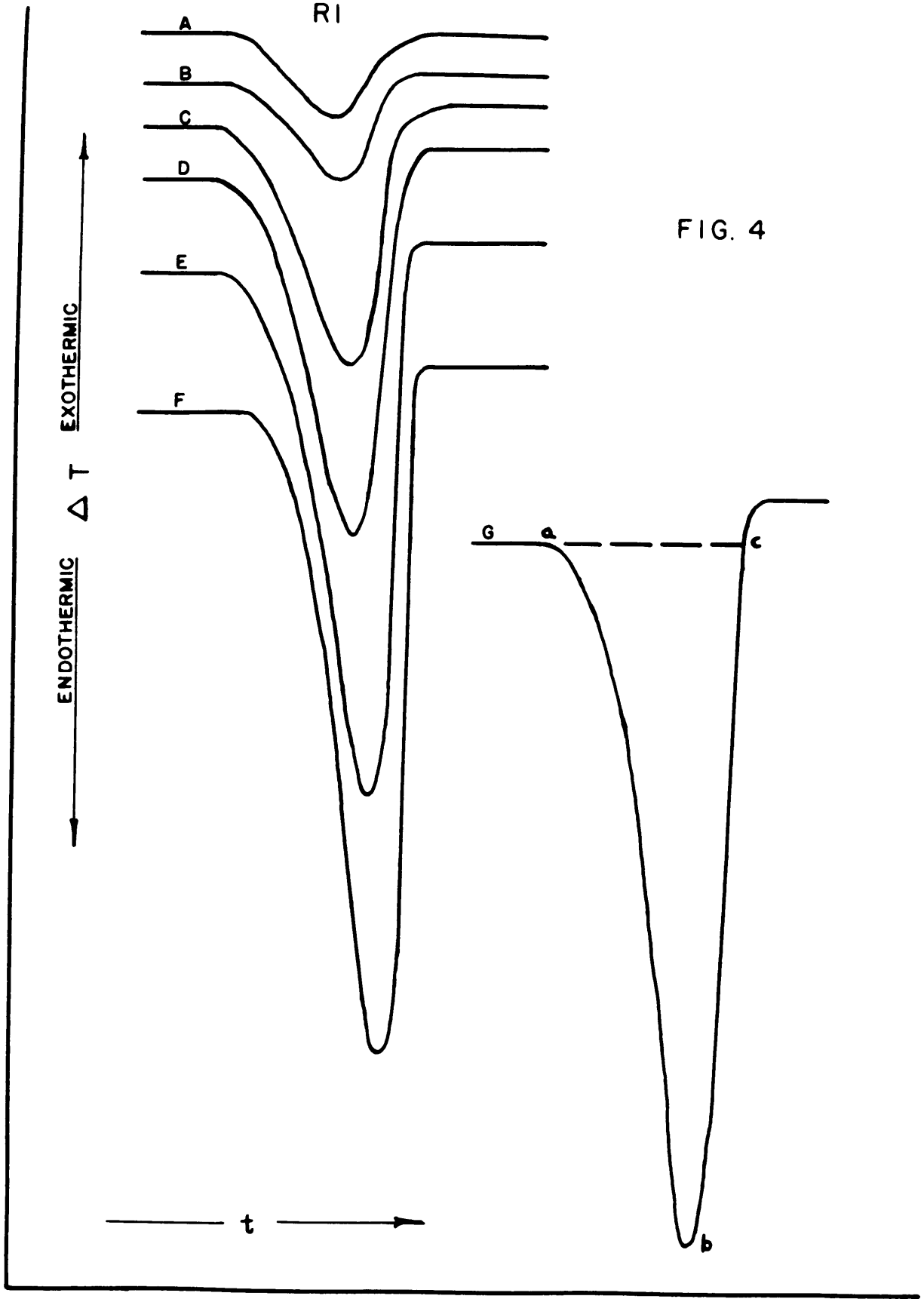
FIG. 4
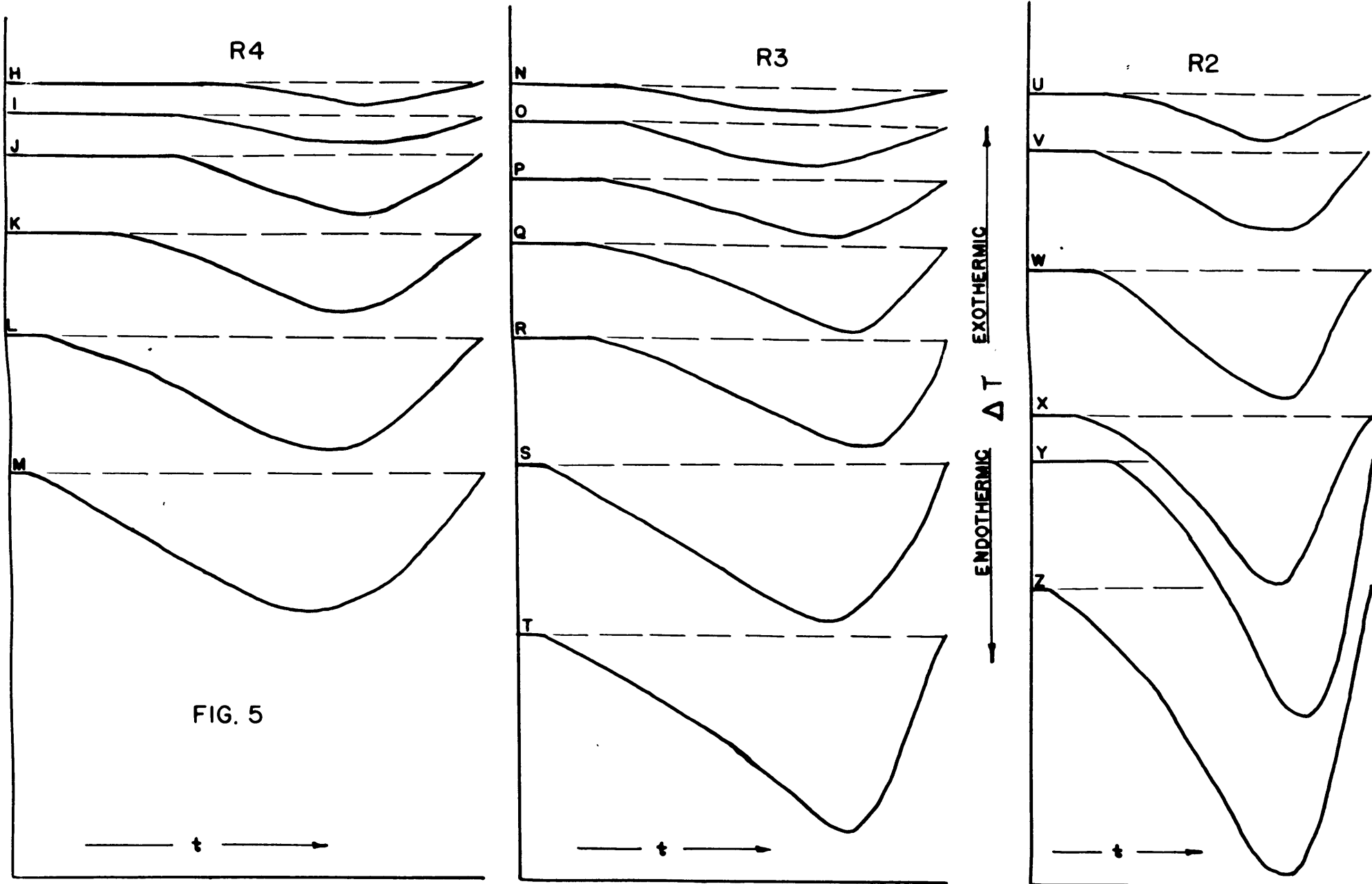
FIG. 5

thermocouples that gives rise to a non-linear base-line. In Fig. 2 point c is often displaced towards point c' and the curve continues towards Y. In addition, slow heating rates (10°C. per minute) decrease the slope of ab so that point a is often very difficult to identify. Although not directly applicable to this problem it has been mathematically and experimentally demonstrated[8] that for periodic heat flow in one direction the slower the variation in temperature the greater the temperature range in the interior of the body. The application of this principle to our case means that slower heating rates increase temperature gradients in the sample which in turn diminish the thermographic response. This is a parallel effect to that of increasing the mass of the sample beyond some critical value, as will be shown later. The thermographic curves for low rates in Fig. 4 clearly display this difficulty and the work of Norton[1] and Berkelhammer[2] emphasizes it.

The difficulties of the non-linear base-line are largely eliminated by reducing the mass of the furnace housing, employing high heating rates (30°C. per minute), and testing small samples of large ΔH. The reaction point a, Fig. 2, is sharply defined as the slope ab steepens, and the base-line deviation is reduced to a small magnitude. The method of area measurement adopted overcame this slight deviation as shown in Fig. 4, curve 6. The base-line is merely extended

from point <u>a</u>, the reaction origin, to point <u>c</u>, where the
reaction is assumed to be completed. The area measured is
that enclosed by <u>abc</u>.

Effect of Temperature Gradients in the Samples

In studies to follow on the amphibole minerals it
became desirable to determine the optimum mass of the sample
to be tested in the analyzer so that the minimum amount of
sample might be used without diminishing the accuracy of
the calorimetric measurements. The previous experiments
already showed that high rates of heating and low mass
samples were features of importance in this matter and so
the 30°C. per minute heating rate was set down as part of
the standard procedure.

Preliminary tests showed that the general range of
ΔH for the reaction[9]

$$Ca_2Mg_5Si_8O_{22}(OH)_2 + \Delta H = 2CaSiO_3.5MgSiO_3 + SiO_2 + H_2O$$

Tremolite   Diop.-clinoenst.   Qtz.
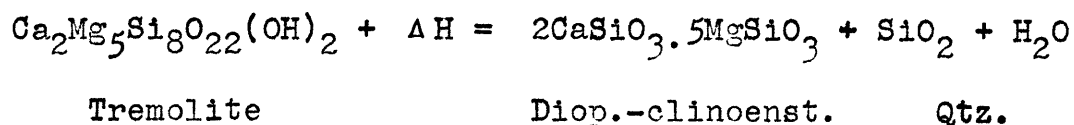
is very roughly 1.00 cal. per 100 milligrams of sample, and
the thermographic response is in the range of 2 square inches
for this reaction. This indicated that smaller samples might
be feasible and so a series of runs was made on a random
specimen in amounts increasing from 20 to 130 milligrams, and

the resulting curves are shown in Fig. 6 and the compiled
data in Table II. The relation between mass of sample and
area is graphically shown in Fig. 7. The plot is clearly
defined and displays a marked departure from linearity
when the mass exceeds approximately 60 milligrams.

The falling off of thermographic response is a
direct result of a temperature gradient within the sample
as the mass exceeds the apparent critical value of 60
milligrams, and consequently, Equation (3) is valid in the
investigation of the amphiboles as long as the critical mass
is not exceeded.

Relation Between Heating Rate and Thermographic Response

A cursory examination of Fig. 3 reveals that some
regular relation exists between the rate of heating and the
corresponding thermographic responses for a given energy
change. In order to obtain a clearer picture of this relation
the following terms are first defined.

From Fig. 3:

$$Area = A$$

$$Q = Q$$

$$\theta = \tan^{-1} \left(\frac{A}{Q}\right) \quad \text{measured in degrees and tenths on the scale of Fig. 3.}$$

FIG. 6

FIG. 7

MASS (MILLIGRAMS)

REACTION AREA (TENTHS OF SQ. IN.)
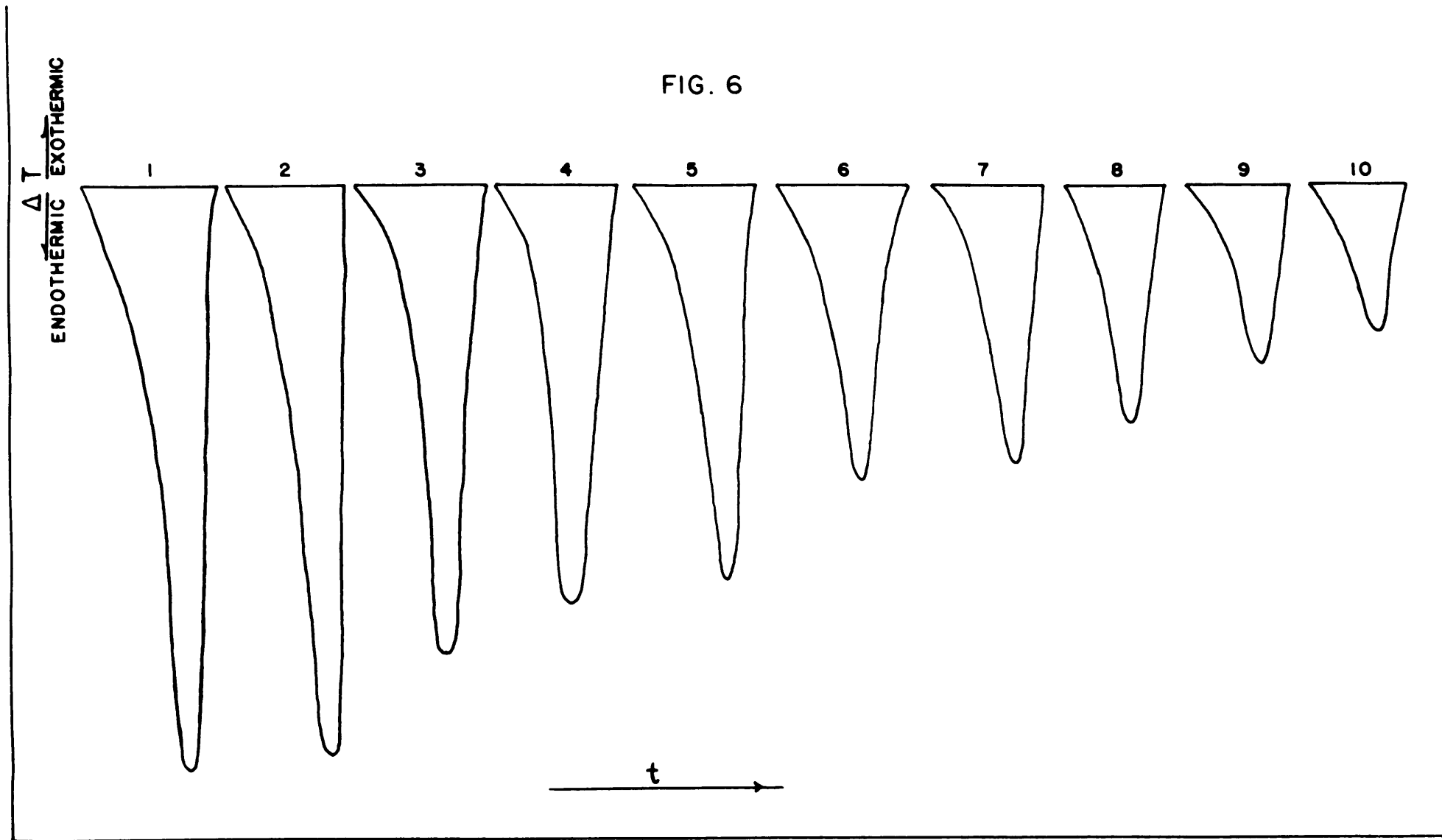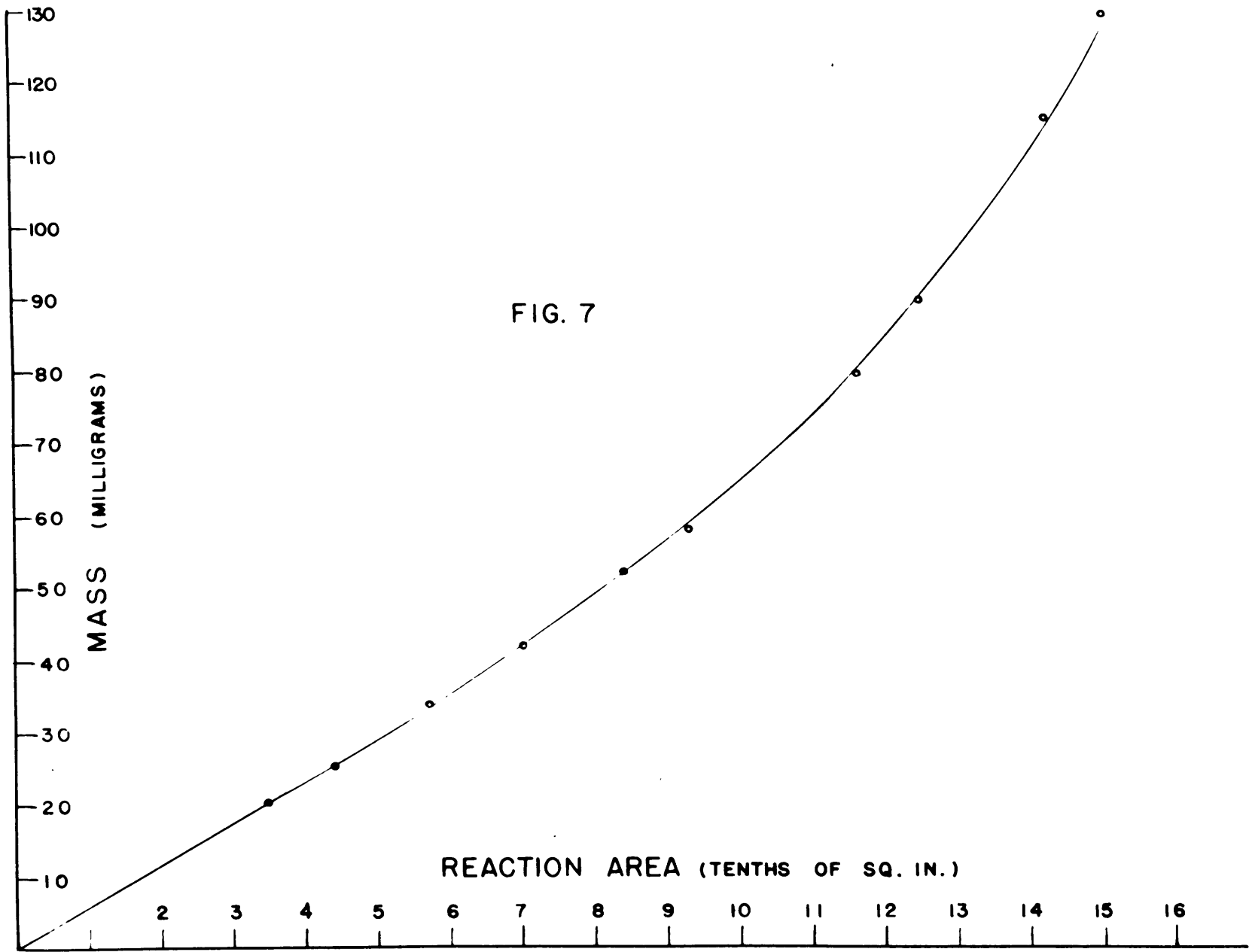
TABLE II

Reactive Sample		Thermographic Response
Sample No.	Weight (mg)	Area (Sq. In.)
1	130	1.50
2	115	1.42
3	90	1.25
4	80	1.16
5	58	0.93
6	52	0.84
7	42	0.70
8	34	0.57
9	25	0.44
10	20	0.35

Rate of heating = R

$$Q = \frac{A}{\tan \theta} \qquad (4)$$

The use of units in the above terms are prohibitive in the derivations following, obviously, because the numerical values are strictly relative, e.g. square inches versus calories in Fig. 3.

The graphical representation of R and θ in Fig. 3 indicates that some form of exponential relation exists between these two functions. A plot of R versus θ (Fig. 8) as compared to the plot of e^x against x verifies this observation. The values for R and θ are tabulated below.

R	θ
10	30.17
15	34.50
22.5	36.00
30	36.92

We shall now proceed to find the relation between R and θ so that some function of R can replace θ in Equation (4). The solution of this relation is carried as follows:

$$R = e^{\theta/k} \qquad (5)$$

$$k \ln R = \theta \qquad (6)$$

FIG. 8
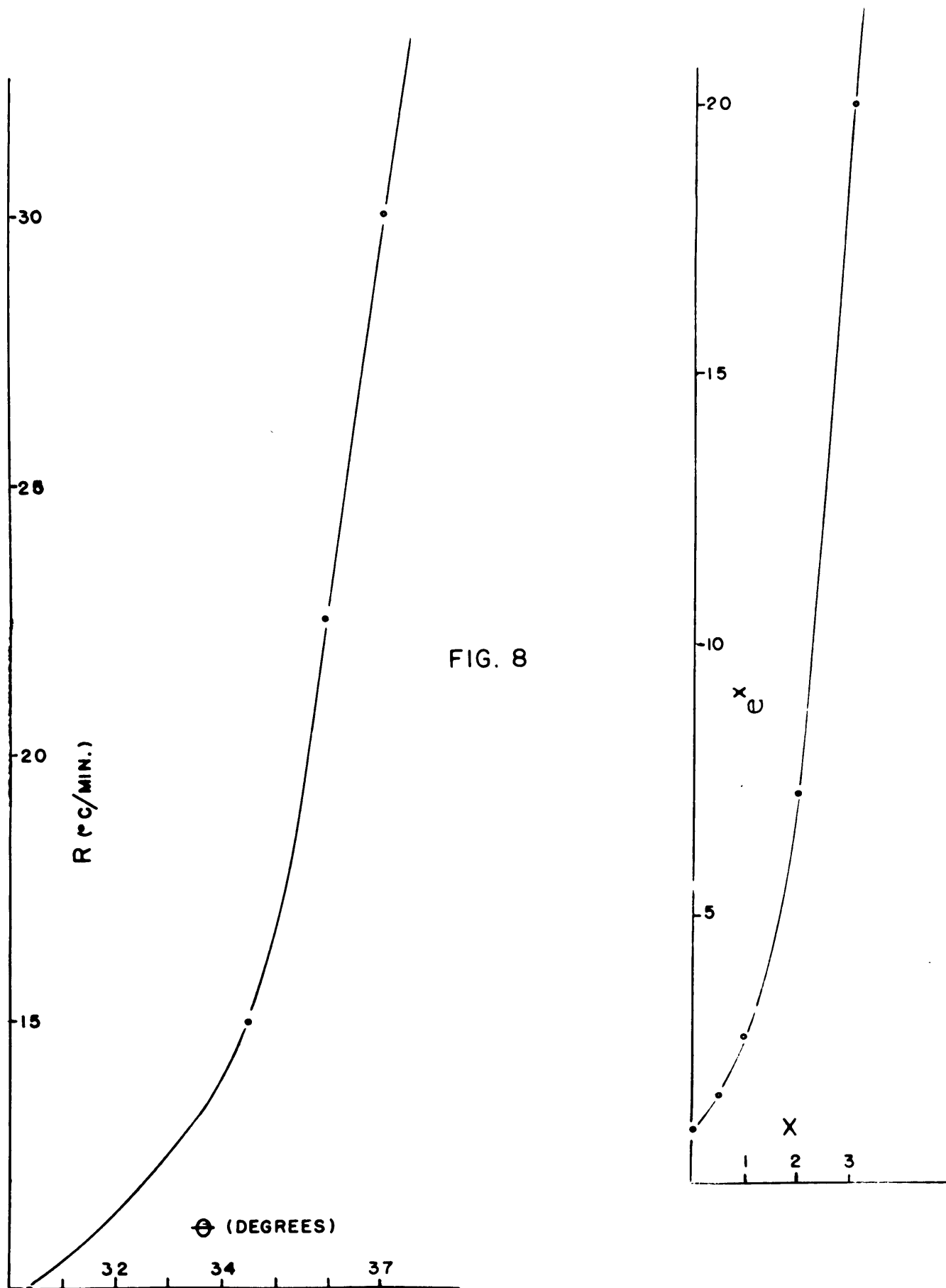
Note: k here is not to be confused with k in Equation (1). Substituting the above values of R and Θ in Equation (6) and solving for k we find,

R	Θ	k
10	30.17	13.13
15	34.50	12.78
22.5	36.00	11.58
30	36.92	10.82

It is seen that k is not constant, but rather a variable that decreases as R increases. As a result another substitution must be made for k so that a more general term can be substituted for Θ. Continuing the empirical derivation, a plot of R versus k (Fig. 9) shows the general form

$$y = mx + c$$

where R and k are y and x respectively

or,
$$R = mk + c$$

and,
$$k = \frac{R - c}{m} \tag{7}$$

Substituting for k in Equation (5) we have,

$$R = e^{\frac{m\Theta}{R - c}}$$

$$\ln R = \frac{m\Theta}{R - c}$$

and,
$$\Theta = \frac{\ln R \,(R - c)}{m} \tag{8}$$

R = mK + C
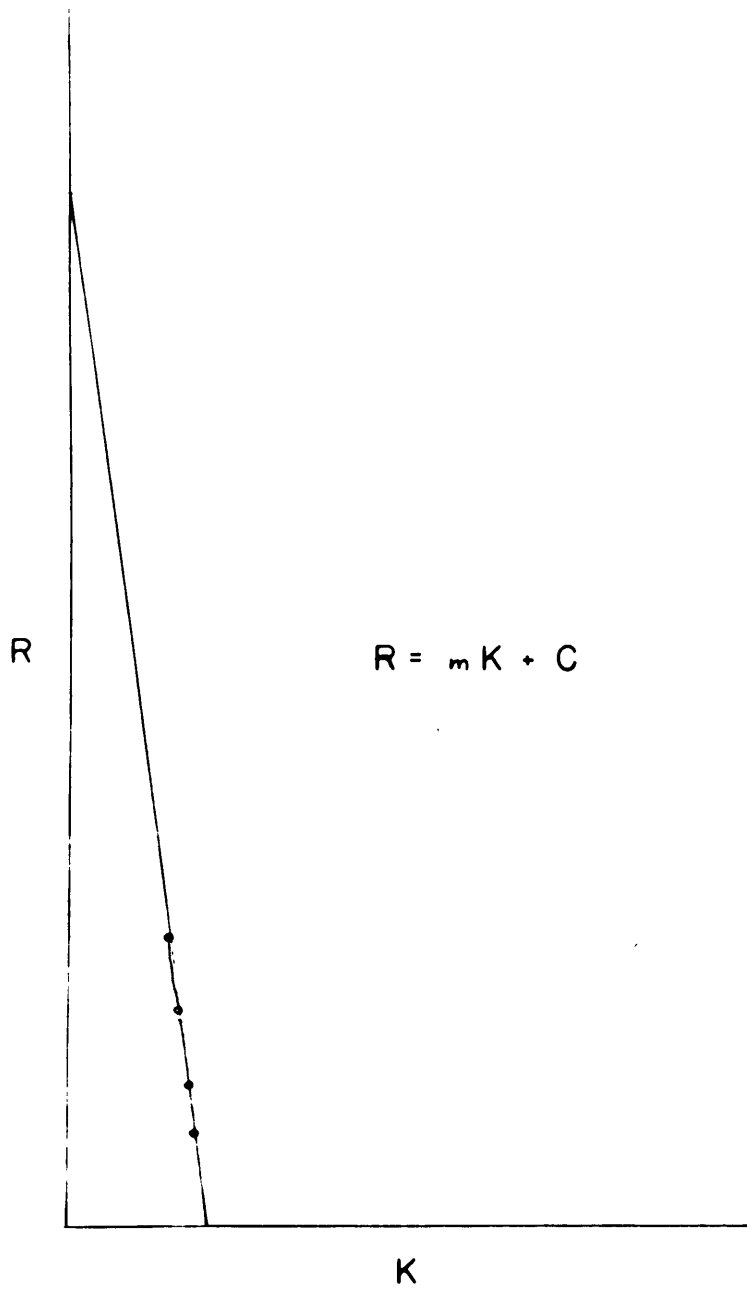
FIG. 9

where,
$$m = 8.10$$
$$c = 117.50$$

We now have an expression for θ in terms of R and the constants m and c, and a final substitution in Equation (4) gives

$$Q = \frac{A}{\tan \left(\frac{\ln R \, (R-c)}{m} \right)} \qquad (9)$$

Equation (9) is the expression for calorimetry determinations using the apparatus described in this investigation. Since the derivation of this equation is empirical it is necessary to restrict its validity for the range of heating rates of 10°C. to 30°C. per minute.

General Discusion

The results of these experiments support the contention of the importance of a low-inertia radiation-type furnace in investigations of this nature. The sensitivity of the instrument was found to be 30 to 100 times greater than those described in the recent literature[1],[2],[3],[10],[11] and it should be emphasized that no amplification was needed to achieve the highly magnified thermographic curves. Increased sensitivity, however, carries with it the increased hazards of technique and so a strict procedure of analysis

must be set down and followed. The symmetry of the housing is of utmost importance in this respect. Exact centering of the sample block and the thermocouples within it are crucial points in the technique. The thermocouples themselves, in the differential circuit, must be well-matched and uniform. Packing of samples and careful grain-sizing are also important constants of the technique.

It has been repeatedly mentioned here that the high rates of heating are an ideal feature of the analysis, but it should also be noted that this results in a prolonged life for the furnace which is most desirable. On the other hand, it should be pointed out that these high rates are poorly controlled below 300°C. and are, therefore, not useful in the low ranges. In addition, high cooling rates are difficult to maintain.

It is suggested that further diminution of the furnace and sample housings to ones having still lower inertias may make possible calorimetric studies over a wider temperature range. The possible applications of such a calorimetric tool are numerous.

PART II

A STUDY OF SOME AMPHIBOLES

SECTION A - ANTHOPHYLLITES

SECTION B - THE MONOCLINIC AMPHIBOLES

Introduction

The amphiboles, like many of the other common rock-forming mineral groups, form a very complex suite not easily classified, largely because of their highly variable chemical composition. This investigation is an attempt to correlate the chemical composition and crystal structure with the thermal characteristics of some selected types.

Three major tools for analysis are employed: (1) differential thermal analysis, (2) chemical spectroscopy, and (3) x-ray powder diffraction. The first of these methods is used to detect and measure such thermal characteristics as expulsion of $(OH)^-$, oxidation of ferrous iron, and heats of reaction and dissociation. The second and third techniques are identification studies which are closely related to the thermal experiments. The results of the three methods are evaluated with respect to each other in the correlation.

The temperature range selected in the investigation is 600°C.-1125°C., since temperatures below 600°C. lie in the field of stability of the amphiboles, and are therefore unimportant to this study. Between 600°C. and 1125°C. all of the above-mentioned changes occurwhich are well-suited to the range of the differential thermal analyzer, which is operated at heating rates of 30°C. per minute, with a furnace evacuated to pressures of 1 mm. Hg.

The study is divided into two parts on crystallographic grounds. The first part is the examination of the orthorhombic anthophyllites, and the second part deals with the large group of monoclinic amphiboles.

SECTION A

Anthophyllites

Previous Investigation:

The crystal structure of anthophyllite was described by Warren[12] who gave the general formula $(Mg,Fe)_7Si_8O_{22}(OH,F)_2$, and showed the now-familiar double-chain silicate structure, and its relation to the single-chain orthopyroxene.

An exhaustive chemical-optical investigation of the group by Rabbitt[13] expanded the general formula to $X_7Y_8O_{22}(OH,F)_2$, where X is chiefly Mg,Fe^{++} and Al and in minor part Mn^{++}, Ti^{++++}, Fe^{+++}, Ca^{++}, Na^+, and K^+. Y is chiefly Si^{++++} and in part Al^{+++}. The maximum amount of Al is $(Mg,Fe)_5Al_2$ in X, and (Si_6Al_2) in Y. Fe^{++} reaches a maximum of about $(Mg_{3.5}Fe_{3.5})$ in X. His investigation also included some differential thermal analyses from which he noted the simultaneous loss of structural $(OH)^-$ and oxidation of ferrous iron, these reactions being endothermic and exothermic respectively. Weight loss determinations led him to conclude that H_2O is not easily removed at 1000°C. or even 1100°C. The results of Rabbitt's thermal experiments are

reexamined in the present investigation and will be demonstrated later.

In a study of the system[14] $MgO-SiO_2-H_2O$, the stability of magnesian anthophyllite was shown to be closely related to the presence of water vapor in limited concentration. Enstatite forms when insufficient water is present, and the more hydrous phases, talc and serpentine, crystallize in the presence of excess water vapor.

The role of $(OH)^-$ in magnesian anthophyllite was shown by Thilo[15] as an expulsion of hydroxyl groups in the form of H_2O at 800°C., with subsequent structural breakdown at 900°C. according to the reaction

$$Mg_7Si_8O_{22}(OH)_2 + \Delta H = 7MgSiO_3 + SiO_2 + H_2O$$

anthophyll.   enstat.   qtz   (10)
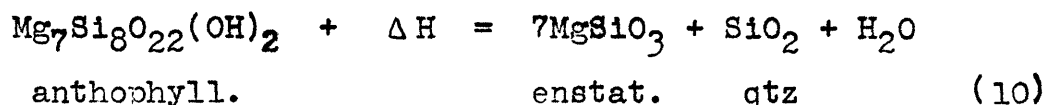
Thilo's[15] dehydration plot shows a weight loss of 2.3% in Fig. 10, the theoretical H_2O content of magnesian anthophyllite being approximately 2.2%.

Present Investigation:

Hydroxyl in anthophyllites:

The dehydration of magnesian anthophyllites described above was performed by the static method of maintaining constant temperature until constant weight was attained. Since the

FIG. 10
DEHYDRATION CURVES
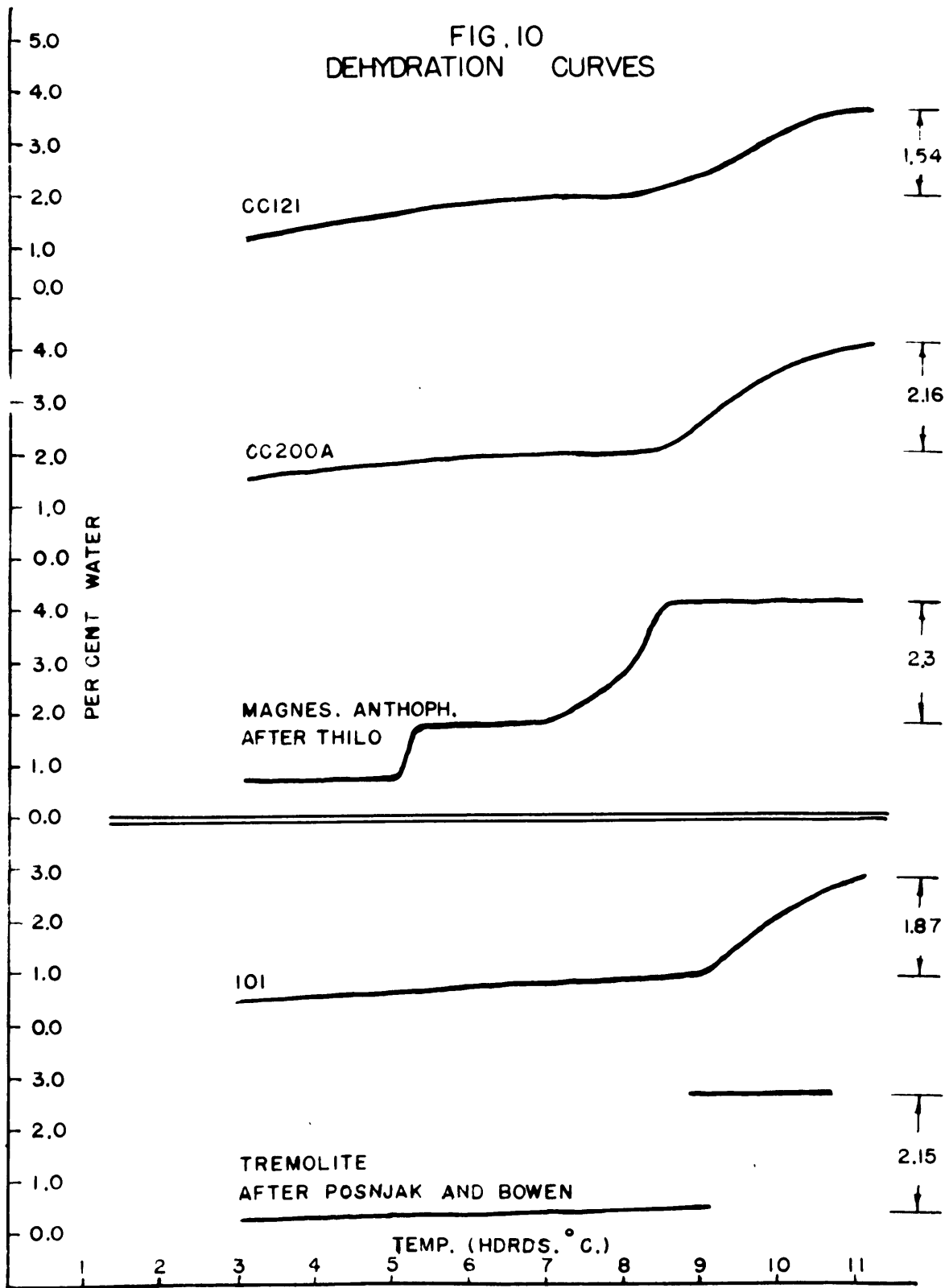
thermographic curves of the differential thermal analyzer are the result of dynamic changes, they are interpreted differently from curves involving static changes. In effect, this means a lag should be expected in the thermographic record of the dynamic experiments.

Weight loss experiments on two anthophyllites, CC200A and CC121, by the dynamic method, are compared with the static test by Thilo in Fig. 10. The method in this investigation simply involved heating to a desired temperature, immediately cooling and placing in a dessicator, and weighing. The results clearly indicate a reaction temperature lag by the dynamic method. Water is still being removed above 1000°C. but appears to be completely driven off by 1100°C. Although the expulsion begins at 800°C., x-ray powder diffraction patterns reveal no structural breakdown of the material until 975 ± 20°C., when most of the hydroxyl groups have been removed. It is likely that the reaction takes place in two steps that overlap in the region of 975°C.

First, $\quad Mg_7Si_8O_{22}(OH)_2 + \Delta H = Mg_7Si_8O_{22}(O) + H_2O \quad (11)$

then $\quad Mg_7Si_8O_{22}(O) + \Delta H = 7MgSiO_3 + SiO_2 \quad (12)$
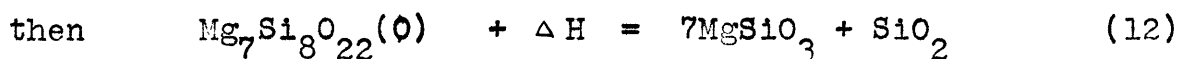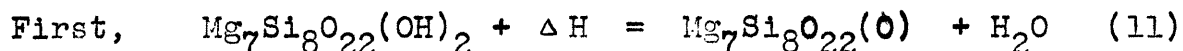
Discussion will be confined in this section to the first reaction above. It is seen that for each pair of hydroxyl ions removed, one oxygen remains to satisfy the valence restrictions. In the hydrous anthophyllite structure each $(OH)^-$

is bonded to $3Mg^{++}$ situated at the corners of an equilateral triangle. Each of these Mg ions completes its octahedral coordination with the unshared oxygen ions of the silicon-oxygen chains. Two $(OH)^-$ per mole removed from the hydrous form would result in a rupturing of the bonds of only one-twelfth of the anions in the structure. To be sure, a few octahedra of Mg-O-OH result in a slightly unbalanced co-ordination in the anhydrous form described above but the change is too slight to be identified by ordinary x-ray powder diffraction methods. From this, it seems safe to assume that the breaking of the hydroxyl bonds in itself is not sufficient to alter the crystal structure to any marked degree.

An examination of the dehydration curves reveals a disparity between the chemical analysis for H_2O and the weight loss determinations. The chemical analyses for H_2O in CC121 and CC200A are 1.48% and 1.59% respectively, and at first observation appear to be about 25% too low. One might expect low results in the chemical analysis for such minute amounts, but two other possibilities must be borne in mind. First, the theoretical weight per cent value of H_2O drops from 2.2 in the pure Mg types to 1.8% in the non-existent pure Fe^{++} types. In practice then, we should find only about 1.95% to 2.15% in the ferrous types depending on their FeO content. Secondly, fluorine may be present in the group $(OH, F)_2$ in partial or complete replacement of the hydroxyl. A more

complete discussion of the role of fluorine will be given in
another section, but it may be briefly mentioned here that
the fluorine is not removed with the hydroxyl and the
resulting weight loss determinations of highly fluoriferous
specimens may be extremely low. The original chemical analyses
showed no fluorine in either of the two specimens, but since
this method is unreliable for such small quantities, the
fluorine was redetermined spectrochemically by Ahrens[16]
method. A trace was found in CC200A and 0.13%F in CC121.
The atomic weights for $(OH)^-$ and F^- are close enough so that
their percentages may be added directly in the determination
of the $(OH, F)_2$ group. The weight loss determinations for
H_2O plus the new fluorine determinations are tabulated below
in comparison with the original analyses.

	New Analyses		Old Analyses	
	CC121	CC200A	CC121	CC200A
% H_2O	1.54	2.16	1.48	1.59
% F	0.13	tr.	None	----
Total	1.67	2.16	1.48	1.59

The value of 2.16% (H_2O + F) for CC200A is considerably
closer to the correct theoretical value for a low ferrous
specimen. CC121, which contains 14.60% FeO, gives a total of
1.67% for H_2O + F which is closer to the hypothetical value
but still somewhat low.

Now the question arises as to whether the oxidation
of the ferrous iron that occurs simultaneously with the
dehydration process causes abnormally low weight-loss deter-
minations in samples high in FeO. This problem is resolved
by analyzing the two simple expressions below:

$$2(OH) = H_2O + \frac{1}{2} O_2$$

$$2FeO + \frac{1}{2} O_2 = Fe_2O_3$$
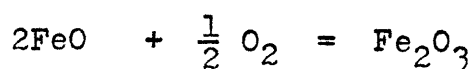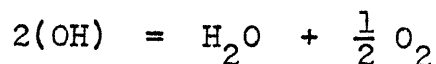
Using one mole of CC121 as a basis, the theoretical H_2O
content should equal 2.0%. Substituting this value in the
first equation above gives a result of 1.6% for the term $\frac{1}{2} O_2$.
This oxygen remains in the structure when the hydroxyl ions
combine to form water. Again, if one mole is used as a basis
for calculation, the second expression above reveals that 1.62%
oxygen is needed to oxidize 14.60% FeO. This gives a value of
1.6% for the oxygen available from dehydration and a value of
1.62% for the oxygen needed in the oxidation of FeO. It is
now readily seen that the weight-loss determinations should
not be low in specimens containing less than 15% FeO, and should
be about 2% in non-fluoriferous members.

Oxidation of ferrous iron:

It has already been mentioned that the oxidation reaction
is simultaneous with the dehydration beginning about 800°C.,
and the thermographic curves of ferrous samples are examined

now with a view towards calorimetric determinations of the
reaction

$$2FeO + \frac{1}{2} O_2 = Fe_2O_3$$
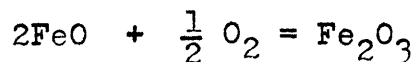
The heat of reaction, H, for the above expression
is (-) 64000 calories per mole Fe_2O_3 at 800°C. The negative
sign indicates the evolution of heat, graphically shown as
an exothermic reaction in the thermographic curves of Fig. 11.
The expression for the free energy change, F, is given below
as

$$\Delta F = \Delta H - T \Delta S \tag{13}$$

where
ΔF is the free energy change at the absolute
temperature T.

ΔH is the heat of reaction per mole at T.

ΔS is the difference in entropy between the
products of reaction and the reactants.

For the reaction of the oxidation of ferrous iron previously
expressed, the free energy equation written above is

$$\Delta F = (-) 64.0 \text{ kcal.} + 26.91 \text{ T} \tag{14}$$

at the temperature 1073°K.

The use of Equation (14) involves the assumption that
the entropies of silicates (17) are equal to the sums of their
constituent oxide entropies. This assumption has been shown
to be substantially accurate for the system $Al_2O_3 \cdot SiO_2$.

FIG. 11 FERROUS ANTHOPHYLLITES
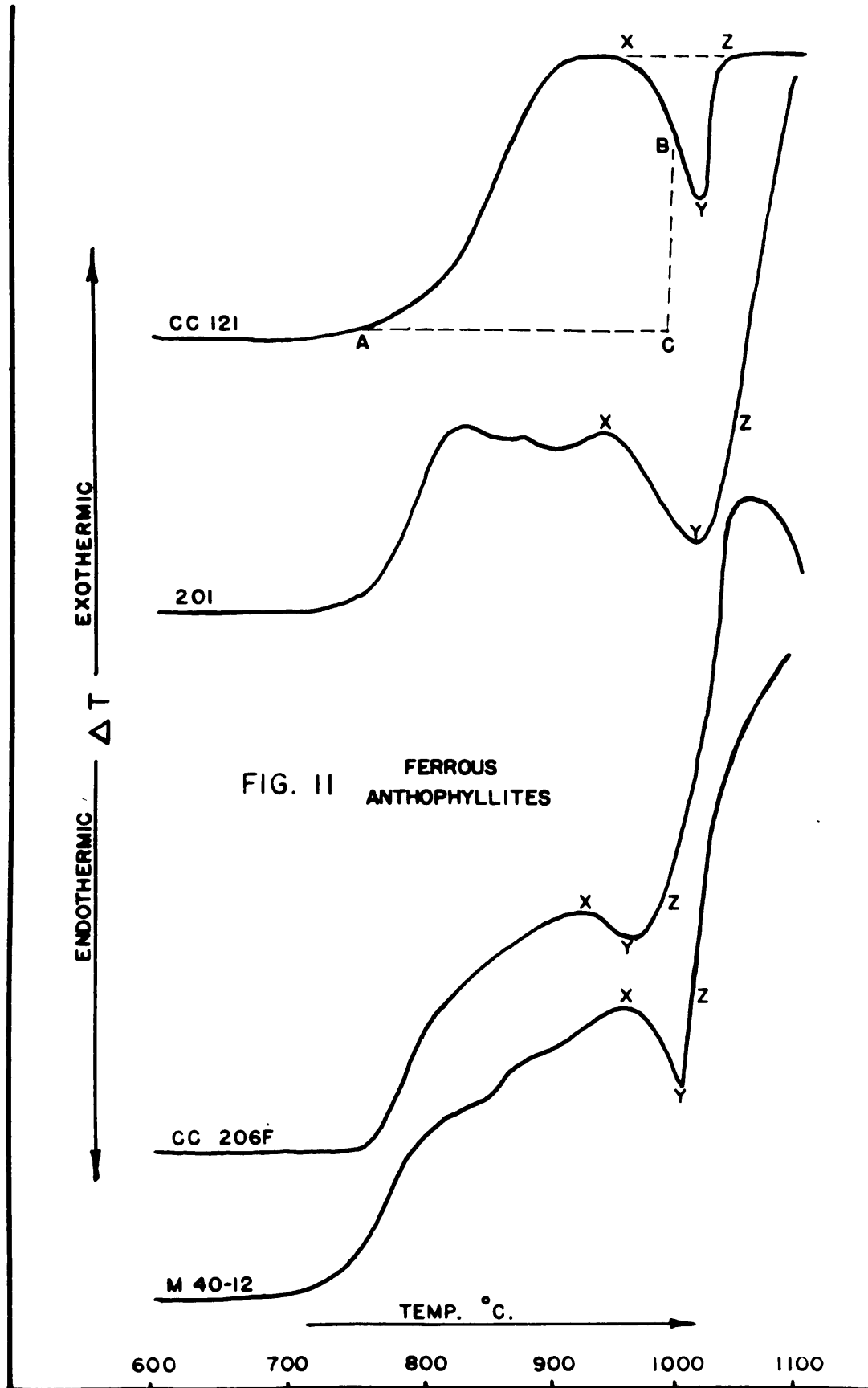
Before employing Equation (14) in these experiments, the accuracy of the calorimetric values must be emphasized. That these are not much better than qualitative is shown by the following:

(1) We assume the oxidation to take place at 800°C., whereas actually it takes place over a probable range of 700°-1000°C.

(2) Accurate chemical analyses for FeO require care and these analyses may be accurate only to within 25%. An interlaboratory investigation[18] gave a standard deviation of 0.707 for 30 analyses of FeO in a diabase, and a standard error of 0.15. The extreme values of the 30 analyses were 6.75% and 9.36%. The undetected presence of 1% TiO_2 in a specimen containing 10% FeO may diminish the accuracy of the FeO determination by more than 10%. However, TiO_2 determinations are not omitted in modern analyses and should be fairly accurate.

(3) The range of (1) embraces parts of two or more reactions and this results in a thermographic response that is difficult, if not impossible, to interpret. The additional reactions include loss of H_2O, collapse of the amphibole structure, possible inversions, and the possible oxidation or reduction of other constituents such as Mn.

The heat evolved from the oxidation of the ferrous
iron in each of the four samples shown in Fig. 11 was
experimentally determined from the thermographic curves in
the following manner. The reaction was assumed to take
place over the temperature range 750°C.-1000°C. and the
areas under the curves were measured by extending the
base-line parallel to the zero-line from 750°C. to 1000°C.
and then vertically from this line to intersect the curve.
The area measured for CC121 is enclosed by ABC as shown
in the figure. It will be noted that another reaction
is occurring in the range near 1000°C.; nevertheless the
method of measurement adopted seems best under the
conditions. Tabulated below are the theoretical values
for the heat of reaction and the experimentally determined
results.

Sample	Theoretical $(-\Delta H)$ (calories)	Experimental $(-\Delta H)$ (calories)
CC121	3.89	0.93
201	2.94	0.75
CC206F	4.87	0.97
M 40-12	4.77	0.95

(Experimental determinations of $(-)\Delta H$ give values
about 500% low and can be considered only
qualitatively.)

FIG. 12
MAGNESIAN
ANTHOPHYLLITES
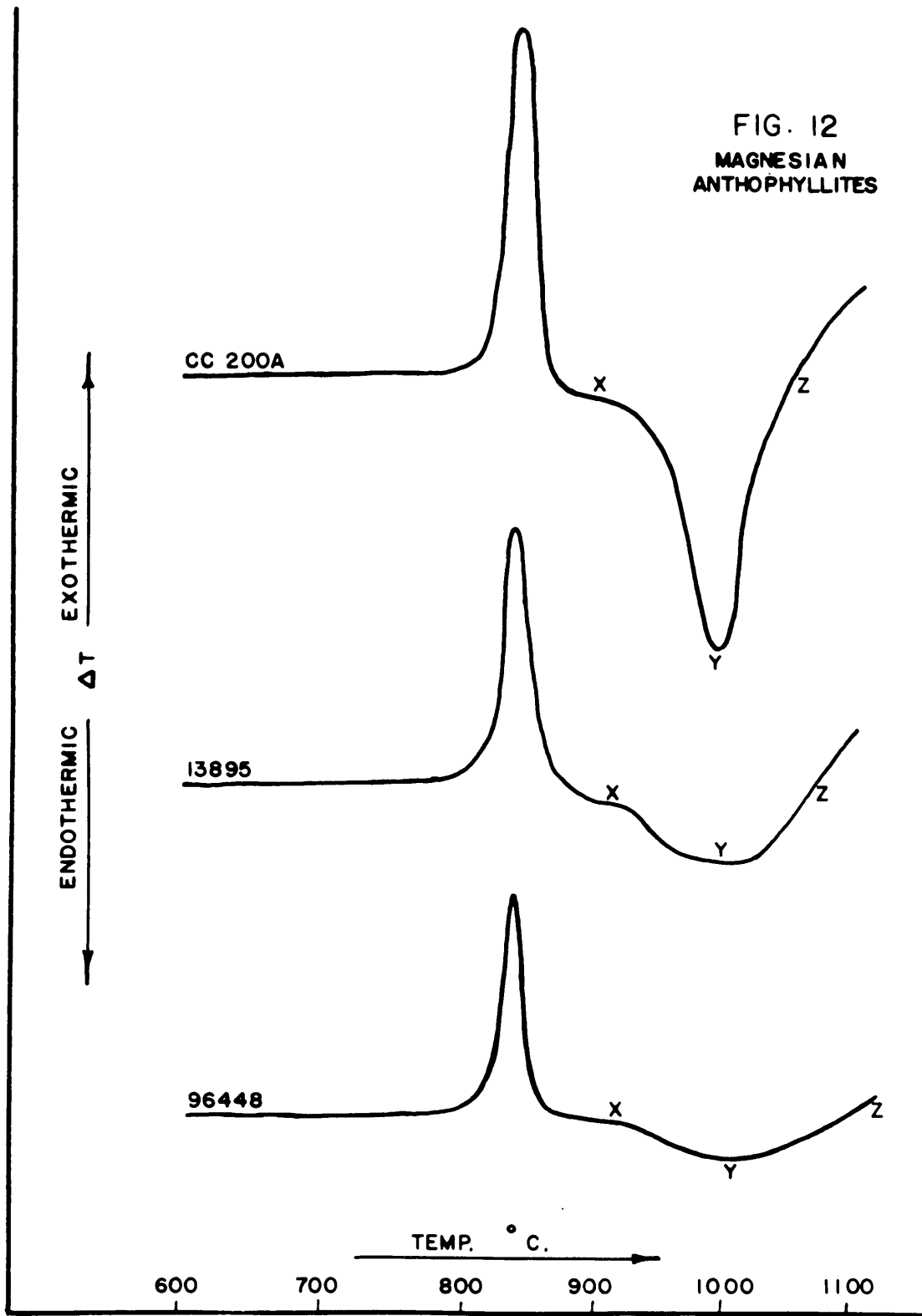
The experimental and theoretical values differ by a factor of approximately 5. It was first thought that these experimental heats were low by the amount of heat absorbed in the dehydration which occurs simultaneously. The thermographic curves for the non-ferrous specimens (Fig. 12) invalidated this hypothesis, however, and another solution was sought.

Energy changes in metals[19], determined by this same method of analysis, also produced low experimental results. It appeared probable, therefore, that the intrinsic nature of the analysis was responsible for the low determinations, and further investigation supported this view. The supporting evidence was gained by testing two different minerals which exhibit oxidation reactions. (1) Olivine was tested as a silicate somewhat akin to the amphiboles with the important difference that its structure does not collapse below 1100°C. (2) Magnetite, which oxidizes[20] at about 220°C. and inverts to hematite at approximately 530°C., was analyzed as a non-silicate example. The thermographic curves for these two minerals are shown in Fig. 13. Semi-quantitative determinations of FeO in these two minerals permitted Equation (13) to be employed again in evaluating the theoretical heats of reaction. The areas contained by ABC, both curves, defined the experimental values for $(-)\Delta H$ and are compared with the theoretical values as shown below.

FIG. 13 OXIDATION CURVES

MAGNETITE

ENDOTHERMIC

ΔT

EXOTHERMIC

OLIVINE

TEMP. (HUNDREDS °C.)

42
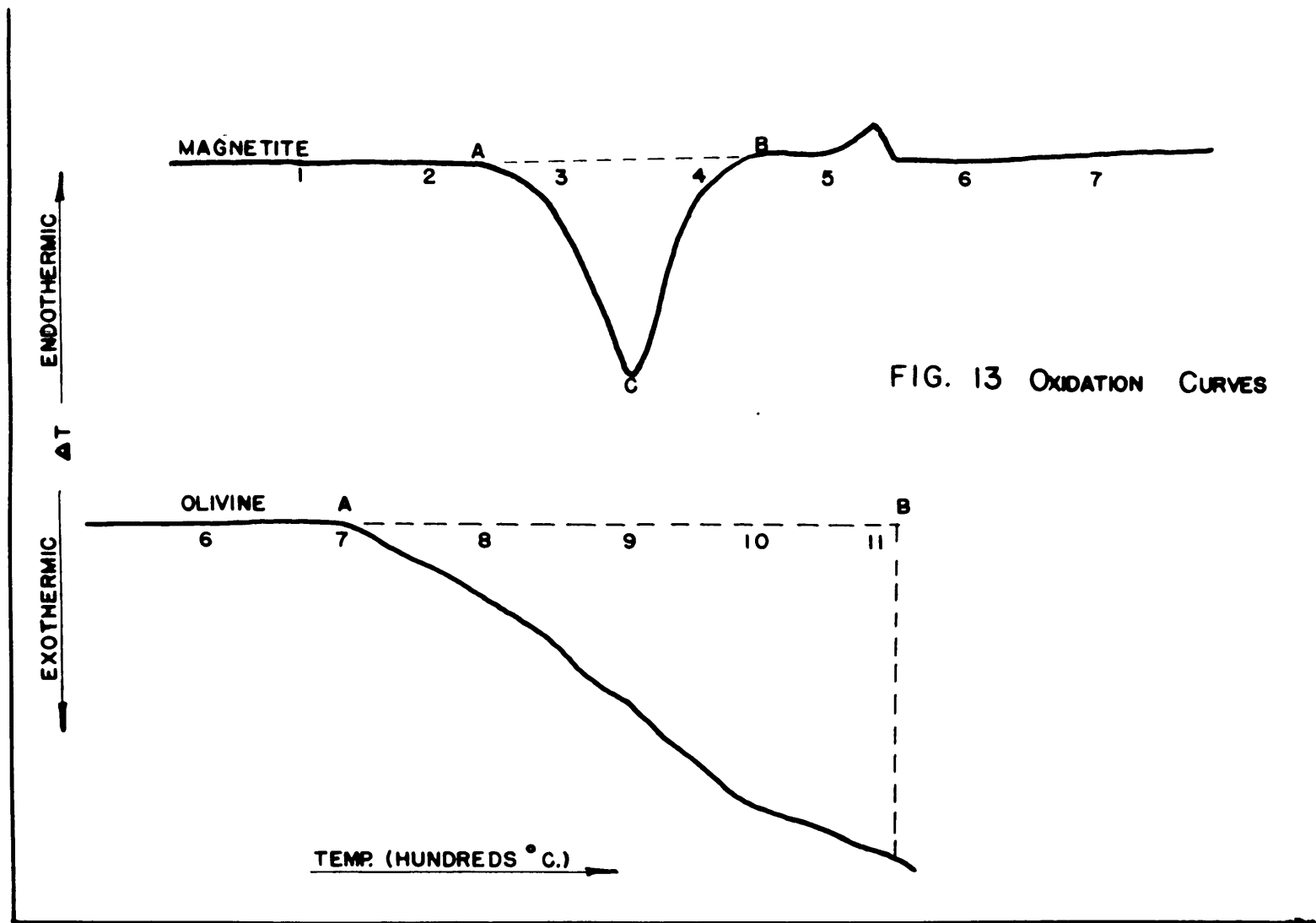
Sample	Theoretical (-) ΔH	Experimental (-) ΔH
Olivine	9.05	1.64
Magnetite	4.68	0.36

As in the amphiboles, the experimental values were found to fall short of the theoretical determinations. The experimental heat for olivine was low by a factor of 5.5, very close to the amphibole determinations. The magnetite analysis differed from the theoretical value by a factor of 13. The fact that olivine gave parallel results to those of the amphiboles emphasizes the conclusions reached in Part I of this investigation. Evidently there is a heat loss amounting to 400-500% in the oxidation reactions of the amphiboles as detected by the differential thermal analyzer. The losses may be attributed to size of sample and, more important, to the large temperature span over which the reaction takes place. These two factors mask the thermographic response considerably, and, since they cannot be avoided, result in the very low heat determinations described. From the qualitative evidence obtained in these experiments, it is clear that the assumptions used in the theoretical heat determinations approach validity. It is also evident that energy changes in other silicates will result in low determinations by this method of analysis: (1) if the temperature range of reaction is greater than 200°C., and (2) if the change is small, say 2-5 calories per gram.

Heats determined in this manner can be expected to result in values, which are low by a factor of 5.

Disintegration of the Anthophyllite Structure

The simple mechanism of structural collapse of the anthophyllites at about 1000°C. is the double-chain single-chain transformation from ortho-amphibole to ortho-pyroxene. The close relation of the amphibole and pyroxene structures makes the reaction possible in the solid state, whereby the entire amphibole framework disintegrates into simpler structural units stable at these elevated temperatures.

Magnesian varieties:

The chemistry and physical nature of the disruption in magnesian specimens reflects the original chemical composition very closely. More explicitly, since the number of different elements in these varieties is small, it is found that the breakdown products are therefore simple in composition, and result from solid state reaction. It was noted that an original 200 mesh amphibole powder transformed into reaction products which were still part of the original powder. This material did not melt, fuse, or cohere. The powder fragments remained free of one another as if each grain reacted by itself, the double chains splitting into the single

chains that form the backbone of the pyroxene structure, and the excess silica tetrahedra forming quartz. The external form of each amphibole grain was maintained throughout the reaction.

CC200A, 13895, and 96448 are the three magnesian varieties of anthophyllite described in this investigation and their thermographic curves are shown in Fig. 12. The endothermic peaks beginning about 930°C. identify ΔH in Equation (10)

$$Mg_7Si_8O_{22}(OH)_2 + \Delta H = 7MgSiO_3 + SiO_2 + H_2O$$
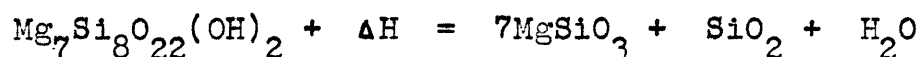
Since the same weight of sample was employed in all these thermal experiments (60 milligrams), it is apparent by examining the thermographic curves that the values for ΔH will vary from sample to sample. In addition, it may be noted that the velocity of the reaction is also different as determined from the slope of XY. Reaction velocity increases with the slope of XY, where X,Y, and Z are defined as reaction points for origin, peak, and completion, respectively, and ΔH is computed from the area XYZ. The heats of reaction in Equation 10 are tabulated below.

Specimen	(+) $\Delta H \pm 15\%$ cal. per gm.	Y peak temp. ($\pm$ 15°C)
CC200A	4.50	995°C
13895	1.67	1000°C
96448	1.50	1010°C

Specimen 13895 gives the most reasonable results because its
composition comes very close to that of a pure magnesian
anthophyllite. 96448 is a fairly pure magnesian sample also,
but it is a fibrous form that cannot be analyzed as easily
as the more crystalline varieties. CC200A is not a true
magnesian specimen since it contains 6.80-8.71% FeO (two
analyses). Rabbitt's[13] thermographic curve for CC200A was
described as "a vague continuing loss... of H_2O at 1050°C".
From the present investigation it is seen that his interpre-
tation overlooked the fact that a more extensive reaction
was taking place [Equation (10) .]

Since none of the specimens contained fluorine, we
assumed that all contained a full complement of water, and
this established a basis for comparing structural breakdown
with chemical composition. It is seen that the lower con-
centrations of FeO are found in samples requiring the least
energy to break the bonds. Conversely, the greater the
content of FeO the greater the reaction velocity. The last
inference may be obtained in two ways, either by noting the
slope of XY, or by measuring the reaction range temperature
XZ. There are no major thermal changes in any of the magnesian
samples following complete breakdown at Z. Apparently the
thermal properties, such as conductivity and specific heat
capacity, are quite similar for the original mineral and its
reaction products. This is to be expected in view of the
previously described "uni-grain" reactions.

Ferrous varieties:

The features of structural disintegration in these specimens parallel those of the magnesian varieties but the mechanism of breakdown is not as simple in the chemically complex ferrous-bearing samples. Most important is the substitution of large amounts of Al_2O_3 and of small amounts of alkalies such as Na_2O and Li_2O.

Once again the products of reaction are orthopyroxene and quartz according to the reaction

$$\begin{vmatrix} Mg \\ Fe^{++} \\ Al^{+++} \end{vmatrix}_7 \begin{vmatrix} Si \\ Al \end{vmatrix}_8 O_{22}(OH)_2 + \Delta H = \begin{vmatrix} Mg \\ Fe^{+++} \\ Al^{+++} \end{vmatrix} \begin{vmatrix} Si \\ Al \end{vmatrix} O_3 + SiO_2 + H_2O \qquad (15)$$
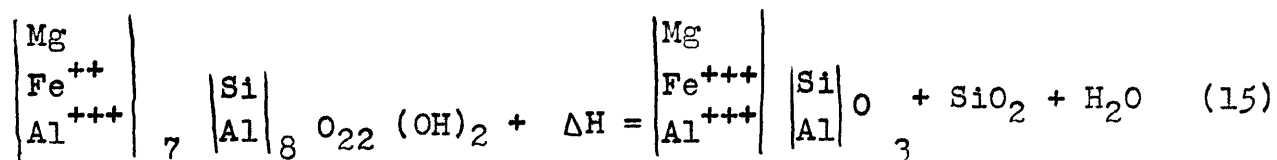
where the orthopyroxene is hypersthene, the variety that accommodates Fe and Al in its structure.

In most cases, the physical nature of the reaction is more complex in that the reaction completion temperature at Z is marked by fusion and sintering. It is believed that the alkalies and fluorine are largely responsible for this fusion which speeds the transformation. Iron also plays an important role here. ΔH, the heat of reaction in Equation (15) is negative as before and varies, as described in the tabulation on the following page.

Specimen	$\pm \Delta H \pm 15\%$ cal. per gm.	$Y \pm 15°C.$ peak temp.
CC121	2.00	1020°C.
201	2.66	1025
CC206F	0.33	990
M-40-12	0.50	1005

Although the order of magnitude of the heats of reaction for
the magnesian and ferrous varieties are comparable, certain
other differences are to be noted. First, it is seen that
the samples highest in iron break down with the smallest
absorption of energy, which is opposite to the effect noted
in the magnesian varieties. The reaction velocities are
extremely high at the reaction origin temperature, responding
in a trigger-like fashion, and disrupting the structure over
a very short span of temperature. X-ray examination reveals
no structural change in M-40-12 at 975°C., but at 1000°C. the
structure collapses in a matter of a few seconds. All the
ferrous samples except CC121 were sintered or semi-fused at
the reaction completion point Z which is marked by a rapid
evolution of heat. It is believed that this sintering may
be caused by a glass-forming reaction of sodium, lithium, and
fluorine, together with small amounts of silicon and aluminum.
No single element may be responsible for these thermal changes,
but the minor constituents of these minerals, namely, the
alkalies and fluorine, (see section on fluorine) show evidence

of being important. The use of alkali fluorides in the synthesis[21] of the amphiboles supports this view. The only single constituent that bears a regular relation to the ΔH's of Equation (15) is alumina, which indicates an inverse relation to the heat of reaction in all four ferrous samples. Larger heats of reaction are found in species containing smaller amounts of Al_2O_3.

Structural Changes in Magnesian Anthophyllites at 800-850°C.

The thermographic curves in Fig. 12 show a major exothermic reaction beginning at about 800°C. and ending at 850°C. This peak is plainly the most noticeable characteristic of the curves for magnesian anthophyllites and is confined to this variety alone. Since the transformation occurs below the temperature for structural collapse, a polymorphic transition might be indicated. The general nature of the reaction peak has the earmarks of a displacive[22] transformation except for the fact that heat is evolved with rise in temperature. Unfortunately, the reaction has not been reversed thermographically. Possibly its nearness to the reaction temperature for structural breakdown, with initial

rupturing of a few bonds, may prevent the reversal. Quenching
experiments have failed to indicate that any high form exists
at 850°C., and this should occur if the transformation is
displacive. The evolution of heat attending rise in tempera-
ture from 800-850°C. can be explained if the mineral is
already in a high form at room temperature. A high form,
stable at this low temperature, however, is very difficult
to explain on thermodynamic grounds.

Additional evidence for a structural change at about
825°C. was obtained by dilatometric tests. A contraction in
the direction of the c-axis was recorded at 830°C., and was
found reversible when the temperature 830°C. was not exceeded.
The method[23] used in the experiments was simple. A single
needle of anthophyllite was observed through a microscope
while in the process of being heated on a platinum resistor.
A scale in the eyepiece enabled the observer to record linear
changes and the temperature was carefully controlled. The
observed shrinkage at 830°C. is 0.44% in the c-axis direction.
The data shown below is in proper sequence (reading downward)
and indicates the reversibility of the transformation.

Specimen	Temp. °C.	Length (c) (any units)
13895	100	45.4
	300	45.4
	500	45.4
	800	45.4
	830	45.2

Specimen	Temp. °C.	Length (c) (any units)
Cont. 13895	775	45.4
	830	45.2
	930	45.4
	1050	45.4

A definite structural transformation of the magnesian antho-phyllites at about 830°C. is indicated by this corroborating evidence. The exact crystallographic nature of the transformation, however, is yet to be established. The heat evolved by the transformation is tabulated below.

Specimen	Heat Evolved cal. per gram
CC200A	3.50
13895	2.84
96448	1.83

The thermographic record for sample 96448 is not suitable for quantitative determinations, as explained previously, and is disregarded in this discussion. The heats evolved by samples CC200A and 13895 must be expected to differ since the first contains 8.71% FeO and the latter contains less than half that amount. The order of magnitude of the heat of transformation of a pure magnesian specimen may be slightly less than the heats shown above for slightly ferrous samples, or about 2.50-2.75 calories per gram.

An interesting feature of the three magnesian varieties examined is that they contain up to 8.71% FeO, and that this relatively large percentage does not interfere or prevent the described transformation from occurring. In conjunction with this observation it is noted that all three specimens are very low in Al_2O_3. The lack of Al_2O_3 perhaps plays an even more important role than the presence of moderate amounts of FeO in the transformation. All these are speculations, however, and must await more conclusive proof.

Fluorine in anthophyllites:

In the discussion of the dehydration of the anthophyllites, it was mentioned that fluorine was not removed from the mineral even at temperatures well above structural collapse (1100°C). Since F is part of the $(OH,F)_2$ group, it may be found in percentages as high as 2.2%, similar to H_2O. Chemical determinations for fluorine in silicates are difficult and may be inaccurate for small amounts. Of the four chemical analyses obtained, only CC206F was reported to have fluorine (0.31%). All seven anthophyllite specimens were examined for fluorine spectrochemically[16] and the determinations are shown in Table IV. The accuracy of these analyses is estimated at ±10%. CC206F gave a new determi-

nation of 0.17%, M-40-12 and CC121 which previously were reported as having none, gave analyses of 0.15% and 0.13% respectively, and all the magnesian varieties showed no fluorine present.

A geochemical analysis of the role of fluorine in anthophyllites cannot be attempted with this small suite of specimens; nevertheless, some definite indications are present even in this small group. The three magnesian varieties, from widely separated localities, contained no fluorine. On the other hand, all the ferrous specimens contained small amounts, although it must be recalled that three of these samples are from somewhat similar pre-Cambrian rocks.

In the discussion on the structural disintegration of ferrous anthophyllites, it was shown briefly that fluorine plays an important role in speeding the reaction velocity of the rupture transformation. In addition, at reaction completion the thermographic records show a large evolution of heat in samples high in fluorine and alkalies. White[24] has shown that Na and K impart very high expansion co-efficients to glasses in which they occur. The formation of the glass or sintered material in itself requires the absorption of heat and often imparts abnormally high specific heat values to materials containing these elements. The expansion effect was observed in the thermal analyzer crucibles at the reaction completion point Z, but the heat absorption is indeed a minor reaction since the thermographic record gives a sharp evolution of heat following Z, and this

completely masks any small endothermic reactions that may be occurring. The formation of the alkali fluoride glass is a heat absorbing reaction, as described above, and should not evolve heat, as the thermographic curves seem to indicate. What is more likely is that the alteration of the powdered material in the analyzer crucible to a sintered or glassy mass largely destroys the analytical value of the thermal record. The relation between the inert and active samples in the crucible is no longer the same when the active sample fuses. In order for the thermal analysis to be truly differential and analytical, the physical character of the inert and active samples must be very similar, that is to say, their thermal conductivities and specific heat capacities must be reasonably parallel. The formation of a glass destroys this parallelism and the thermographic curves record questionable and misleading results. In any event, glass formation around the thermocouple head and leads is highly destructive.

Some Minor Element Determinations:

Among the elements that occur in small amounts in the anthophyllites, we find Co, Ni, Cr, and V, as minor constituents, and Mn, Ti, Li, Na, and F in sub-major amounts. Since spectrochemical methods are well suited to the accurate

determination of low concentrations of these elements, a
semi-quantitative analysis was made of the seven anthophyl-
lites for the nine elements above. Using Rabbitt's[13]
minor element analyses as standards, the analyses are grouped
together here as "minor elements" (Table IV) for correlative
purposes.

At the outset it must be emphasized that seven
specimens fall far short of furnishing a statistical group,
and although the results will be seen sharply delineated,
they must be evaluated in this light.

The immediate and outstanding feature of the results
is the major division between ferrous and magnesian varieties.
Three of the ferrous specimens come from the same type of
metamorphic rock and should therefore be expected to bear
comparable minor element characteristics. On the other hand,
CC200A, a magnesian variety, also comes from the same rock
province as the ferrous samples and this tends to place the
analysis on a more statistical basis. The three magnesian
minerals, it should be noted, come from scattered localities,
and thus make geochemical evaluation more valid.

The higher concentration of Ti^{++++}, Na^+, and Li^+ in
the ferrous anthophyllites is normal. Since Al^{+++} substitutes
for Si^{++++} in considerable amounts in ferrous anthophyllites,
some alkali fits into the structure to satisfy the valence
deficiency. The close association of iron and titanium is
well known.

Vanadium gives an expected correlation. V^{++++} is plentiful in igneous rocks and usually replaces Ti^{++++}, Fe^{+++}, and Al^{+++}. In these anthophyllites vanadium behaves in precisely the same manner.

The transition elements, Co^{++} and Ni^{++}, present one of the more interesting features of the entire analysis. Below are tabulated the ionic radii of the elements important to their interpretation.

Ion	Effective Radius
Mg^{++}	0.78 Å
Ni^{++}	0.78
Fe^{++}	0.83
Co^{++}	0.82

The four elements above have six-fold coordination and therefore can substitute for one another. From radii comparison it is seen that Ni^{++} should follow Mg^{++} more closely than Fe^{++}, and the sharp differences between the magnesian and ferrous anthophyllites makes this observation striking. Ni content has been estimated as high as 0.2% in amphiboles[25]. The three magnesian varieties analyzed all contained no less than 0.1%

Of the sub-major cations only Mn does not follow the expected diadochic replacement in the ferrous varieties.

Mn^{++}, Fe^{++}, and Mg^{++} can replace each other in restricted amounts for they occupy the same site in the structure in octahedral coordination with $(O)^=$ and $(OH)^-$. The effective ionic radii for these cations serve to show that Mn^{++} should be able to substitute for Fe^{++} with more facility than for Mg^{++}. If we consider electrostatic bonding to predominate, then the packing principle indicates that Mn^{++} follows Fe^{++} more consistently than Mg^{++}. The reverse is found in this group of minerals. One possible explanation is that the anthophyllite had to compete with other minerals in the rock for Mn^{++} and the ferrous varieties lost the competition in their rock suites. Another is that the temperature of formation of these ferrous varieties was not favorable for Mn^{++} inclusion and some other mineral captured it. A third is that the Mn^{++} was not available in the original host rock material from which the ferrous anthophyllite formed.

Ion	Effective Radius
Mg^{++}	0.78 Å
Fe^{++}	0.83
Mn^{++}	0.91

The ionic radius of Co^{++} is no deterrent[26] to its inclusion in magnesium structures in preference to iron structures. Apparently Co^{++} behaves as if it were slightly smaller as a result of some covalent bonding, and this aids in its replacement of Mg^{++}. Percentage-wise the Co concentrations are not nearly as outstanding as those of Ni; nevertheless, its correlation is well-established.

Cr^{+++} (0.64A), and the transition elements, fall in the X group of the anthophyllites in six-fold coordination. The geochemistry of Cr^{+++} is characterized[25] by its replacement of Al^{+++} and Fe^{+++} and Mg^{++} despite the valence differences. This latter replacement for Mg^{++} is very apparent in the analyses for two magnesian varieties which gave 0.2% Cr. The high concentration in itself is not common and the additional relation to the magnesian structure needs explanation. Lundegardh[27] has stated that chromium is concentrated in forsterite olivines and is deficient in the fayalite varieties. This may be reflected in the magnesian anthophyllites as a function of temperature of formation where high temperature ferrous iron rejects replacement by chromium, or again, it may only reflect the amount of chromium available and the competitor minerals.

The entire analysis indicates that some broader geochemical relations exist in the anthophyllites that may serve to identify (1) rock characteristics preceding metamorphism, (2) material introduced during metamorphism, and (3) crystallization temperatures.

TABLE III   CHEMICAL ANALYSES — ANTHOPHYLLITES
WEIGHT PER CENT

Spec.No.	SiO$_2$	Al$_2$O$_3$	TiO$_2$	Fe$_2$O$_3$	MgO	FeO	MnO	Na$_2$O	CaO	K$_2$O	H$_2$O	F	Total
CC206F	42.80	17.73	0.49	1.03	15.54	18.32	0.14	1.52	none	0.03	1.94	0.31	99.90
M 40-12	45.98	14.92	0.53	0.62	18.27	17.42	0.04	0.47	0.07	none	1.51	–	99.83
CC121	48.49	13.26	0.41	1.23	20.56	14.60	none	0.11	0.04	none	1.48	none	100.23
201		11.4	0.44	1.04	19.1	10.68	0.19	1.75	0.25	–	1.59	0.21	99.76
CC200A	57.02	1.40	–	–	28.81	8.71	0.09	0.66	1.48			–	
96448		1.25				1.56	.	<0.35	0.32				
13895		0.28				3.35		<0.35	0.36				

ANALYST	TYPE OF ANALYSIS	REF.
F.Gonyer	Chemical	(13)
F.Gonyer	Chemical	(13)
F:Gonyer	Chemical	(13)
F.Gonyer	Chemical	
Author	Spectrochemical	
F:Gonyer	Chemical	(13)
Author	Spectrochemical	
Author	Spectrochemical	
Author	Spectrochemical	

TABLE IV   MINOR ELEMENTS
WT. PER CENT

Spec.No.	TiO$_2$	MnO	Na$_2$O	Li	Co	Ni	Cr	V	F	REMARKS
CC206F	0.49	0.07	2.5	0.06	0.003	0.002	0.0034	0.001	0.17	
M 40-12	0.53	0.06	0.63	0.03	0.006	0.005	0.02	0.03	0.15	Spectrochemical Analyses Determined on a Semi-Quantitative Basis.
CC121	0.44	0.06	<0.35	0.03	0.005	0.004	0.003	0.03	0.13	
201	0.44	0.19	0.71	0.06	0.0031	0.005	0.15	0.03	0.21	Copper Appears in Almost All Specimens in Varying Amounts.
CC200A	0.20	0.13	<0.35	0.006	0.007	0.1	0.2	0.01	none	
96448	none	0.15	<0.35	tr	0.0078	0.1	0.0023	tr	none	Specimen 13895 is Exceptionally High in Copper.
13895	none	0.16	<0.35	tr	0.009	0.2	0.2	tr	none	

SECTION B

The Monoclinic Amphiboles

Previous Investigation:

Thermal studies of green amphiboles were initiated more than fifty years ago by Doelter and Hussak[28] when they determined that hornblende broke down into magnetite plus augite or olivine at a high temperature. During the turn of the century, Des Cloiseaux[29], Belovsky[30] and Weinschenk[31] transformed green hornblende, simply by heating, into basaltic hornblende or brown hornblende. This last phenomenon was examined critically some twenty-five years later by Kozu, et al[32], and Barnes[33]. The two investigations showed a lack of agreement both in experimental results and in conclusions that has not been reconciled satisfactorily. One conflicting result of their respective experiments was the non-conversion of the green hornblende when heated in a hydrogen atmosphere 《Barnes》 , and a successful conversion when heated in a nitrogen atmosphere 《Kozu》 . Barnes concluded that the hydroxyl groups came off as hydrogen, not as water, at the conversion point, whereas Kozu's dehydration experiments indicated the loss of

H_2O at the same temperature. In addition, Kozu reported finding an inversion in these same minerals at $750°C.-790°C.$ by dilatometric tests which identified a contraction in the c-axis direction during this temperature span. One portion of the present investigation is an attempt to clarify the differences on the results obtained by Kozu and Barnes.

Warren[34] determined the crystal structure of tremolite and then demonstrated that the entire suite of monoclinic amphiboles belonged to the same mineral group. The major constituents of the monoclinic amphiboles as given by Warren are listed below in the order of their increasing effective radii and their relation to the general formula $X_2Y_5Si_8O_{22}(OH)_2$:
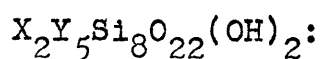
Ion	Effective Radius	Group	C.N.
Si^{++++}	0.39 Å		
		Si	4
Al^{+++}	0.57		
Ti^{++++}	0.64		
Fe^{+++}	0.67		
Mg^{++}	0.78	Y	6
Fe^{++}	0.83		
Mn^{++}	0.91		
Na^+	0.98		
Ca^{++}	1.06	X	8
K^+	1.33		
O^{--}	1.32		
F^-	1.33		
$(OH)^-$	1.4-1.5	(OH)	

Note:

Al^{+++} falls between Si and Y groups,
replacing either

Mn^{++} falls between X and Y groups replacing
either

C.N. = Coordination Number

Using the tremolite formula as the basis for a classification, Sundius[35] derived seven theoretical end-members for the hornblendes. The three fundamental features of his classification are: (1) Al^{+++} substitutes for Si^{++++}, (2) A hole in the structure permits an extra Na^+ to enter, thus raising the sum of (X+Y) to 8. (3) Trivalent cations substitute for divalent cations in Y.

Sundius arrived at seven theoretical divisions for the hornblendes with a major division between the alkaline and lime-alkali varieties as tabulated on the following page:

Tremolite

$Ca_2(MgFe^{++})_5Si_8O_{22}(OH)_2$

Actinolite

Richterite

$Na_2Ca(MgFe^{++})_5Si_8O_{22}(OH)_2$
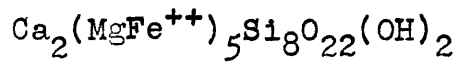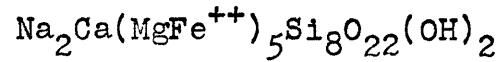
Ferrorichterite

Eckermannite

$Na_3(MgFe^{++})_4(AlFe^{+++})Si_8O_{22}(OH)_2$
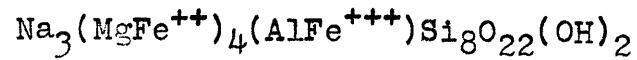
Arfvedsonite

Glaucophane

$Na_2(MgFe^{++})_3(AlFe^{+++})_2Si_8O_{22}(OH)_2$

Riebeckite

Edenite

$NaCa_2(MgFe^{++})_5AlSi_7O_{22}(OH)_2$
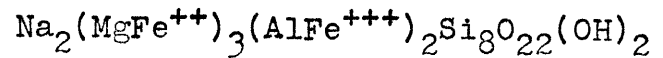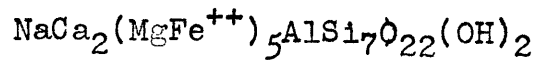
Ferroedenite

Pargasite

$NaCa_2(MgFe^{++})_4(AlFe^{+++})Al_2Si_6O_{22}(OH)_2$
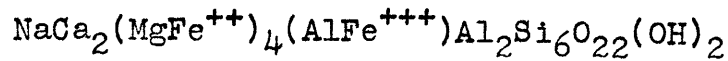
Hastingsite

Tschermakite

$Ca_2(MgFe^{++})_3(AlFe^{+++})_2Al_2Si_6O_{22}(OH)_2$
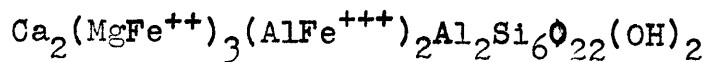
Ferrotschermakite

Posnjak and Bowen[9] demonstrated the role of the
$(OH)_2$ group in hydroxyl tremolite by static weight loss
experiments. At 900°C., the theoretical water content
(2.22%) is removed, and the following reaction takes place
in the solid state:

$$Ca_2Mg_5Si_8O_{22}(OH)_2 + \Delta H = 2CaSiO_3 \cdot 5MgSiO_3 + SiO_2 + H_2O \quad (16)$$

tremolite	diopside – clinoenstatite	crist- obalite
	(solid solution)	
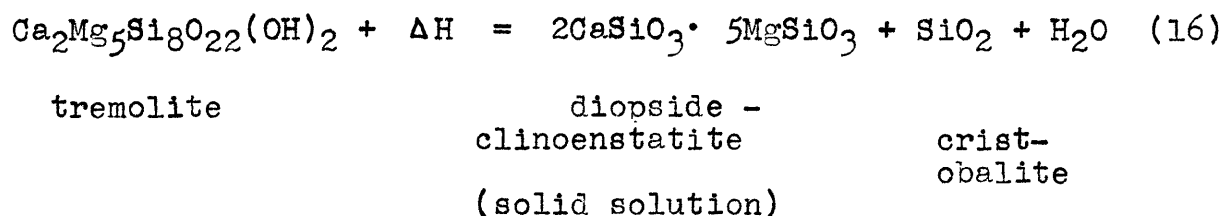
Present Investigation:

Hydroxyl in Hornblendes:

Weight loss experiments, excluding the one described
above, have resulted in odd analyses that demanded peculiar
explanations. Most analyses for water have been low in horn-
blendes for the same reasons that applied to the low analyses
in the anthophyllite group. They are: (1) chemical determinations
are difficult in these low ranges, (2) omission or poor analyses
for the fluorine which belongs in the $(OH,F)_2$ group, and (3)
possible weight gain by oxidation in dehydration experiments..
In addition, Warren[34] has indicated that the $(OH,F)_2$ group
may be partly replaced by oxygen when large amounts of
sesquioxides or Ti^{++++} replace Mg in the structure.

A thermographic record of the removal of hydroxyl groups from specimen No. 204 gives a graphical representation of the dissociation reaction (16) of tremolite. This specimen was a portion of the very pure material investigated by Posnjak and Bowen[9], and is ideally suited for a differential thermal analysis of hydroxyl expulsion. This equation is graphically represented in Fig. 14 (204) by the reaction starting at X and reaching completion at Z . The results are in complete accord with those of Pomjak and Bowen who found the reaction very slow at 900°C. ± 20°C. going only to partial completion after 24 hours at this temperature. Specimens heated to 960°C and immediately cooled showed no structural changes. Evidently the dehydration and monotropic transformation are simultaneous in tremolite, whereas a two-step reaction takes place in the magnesian anthophyllites.

A dehydration analysis, by the same method outlined in Part IIA, was performed on a random specimen of actinolite, (2017), not analyzed previously for H_2O, in order to determine whether it contained a saturated $(OH,F)_2$ group. The result of this experiment was a net weight loss of 1.87% between the temperatures of 900-1100°C. Chemical and spectrographic analyses gave values for FeO.and F of 4.32% and 0.11% respectively. The low content of FeO indicated that no weight gain was to be expected from the oxidation and the fluorine present added to the weight loss determination for water gave a value of 1.98%, (1.87 + 0.11) for the $(OH,F)_2$ group. This value is

FIG. 14
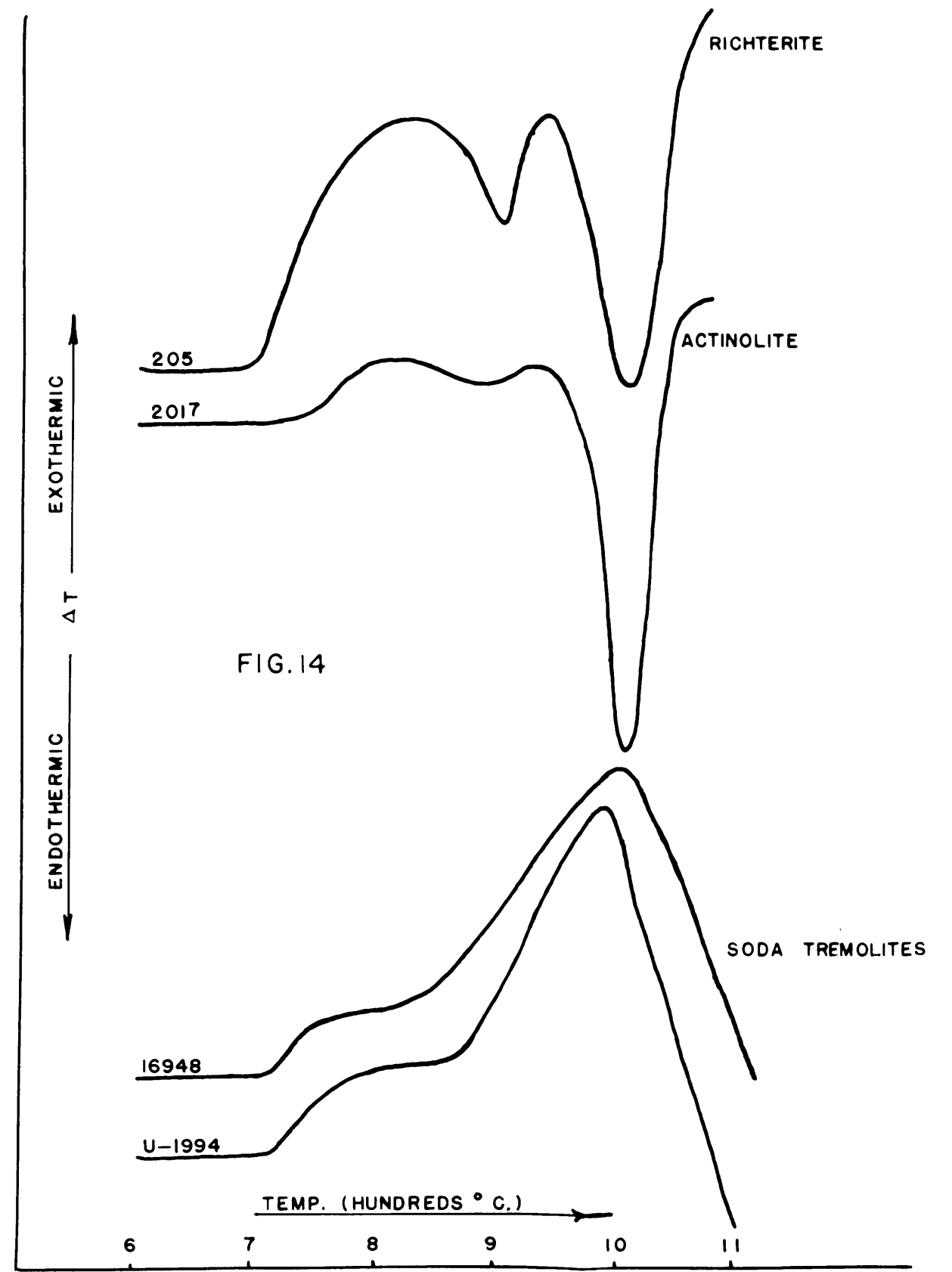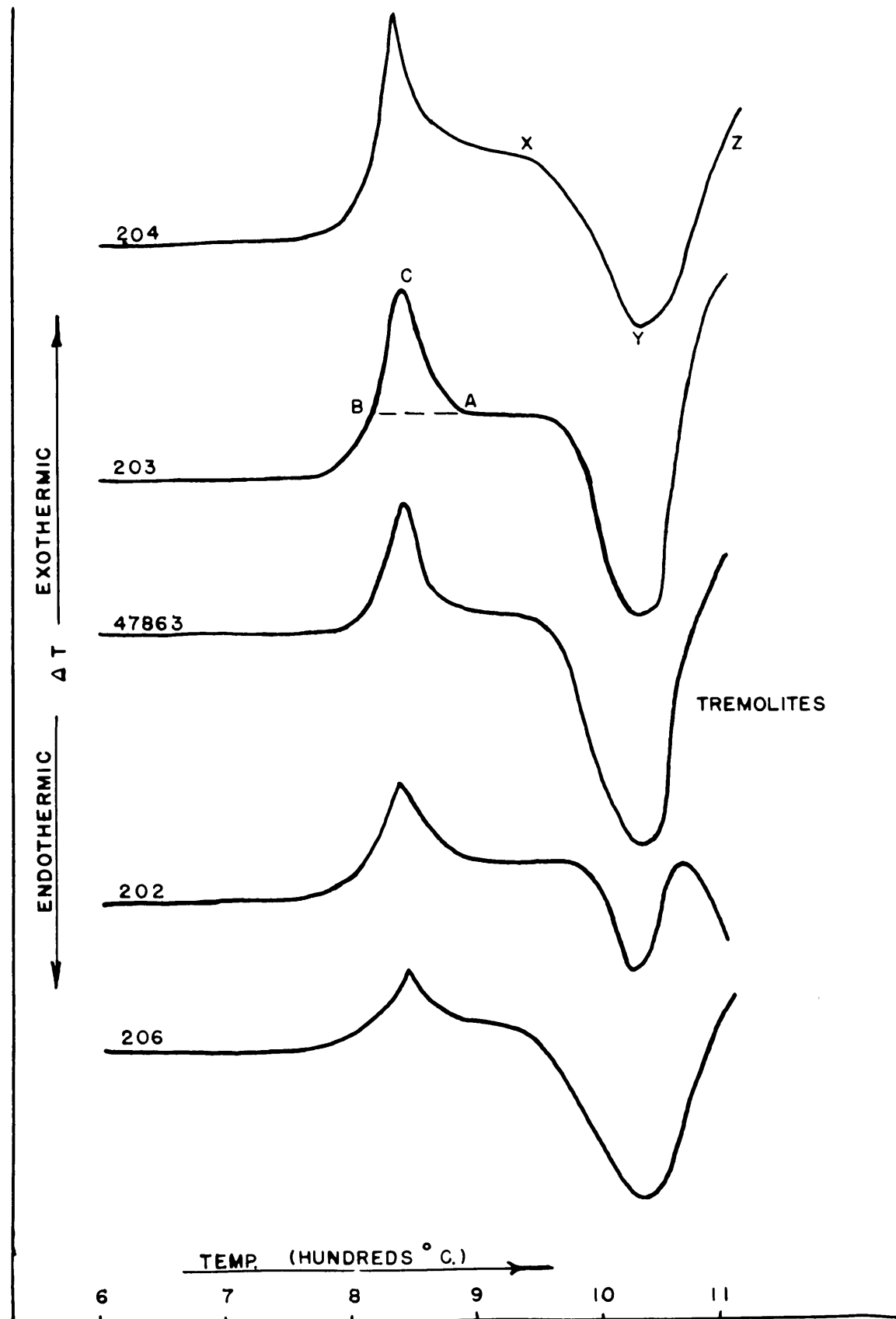
approximately 0.20% lower than the theoretical content of the group; but, in view of the experimental accuracy of the method, it is still acceptable. The main point stressed here is the importance of a fluorine determination in any analysis of a $(OH,F)_2$ group.

Oxidation of Ferrous Iron:

The theoretical basis for the determination of the energy changes in amphiboles due to the reaction

$$2FeO + \frac{1}{2} O_2 = Fe_2O_3$$
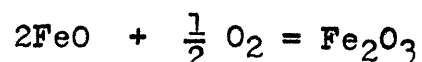
was described in the investigation of the anthophyllites. The assumptions made in the determination of the theoretical heats of reaction $(-)\Delta H$ for the above expression were shown to be substantially valid in that study. As a result, Equation (14),

$$\Delta F = (-) 64.0 \text{ kcal.} + 26.91 \text{ T}$$

the free energy equation for the oxidation reaction alone, was employed in this study also. The heat evolved in the oxidation process was experimentally determined from the thermographic curves in a manner similar to that used in the preceding section.

Two separate experimental heats of reaction were measured for each specimen. In one measurement, the reaction was assumed to take place over the temperature span 750°C - 1000°C. In the other determination, the reaction range was assumed to

cover the temperature span 750°C - Y°C, where Y is the temperature peak for structural collapse. The areas measured for these two determinations shown in Fig. 15, specimen No. 207, are ABC, and AB'Y, respectively. Since the temperature span first chosen (750°C - 1000°C.) in the determination of the heats of reaction was purely arbitrary, it was decided that another might be chosen which would result in energy determinations that would approach more closely the theoretical values. This was the primary reason for extending the temperature range of reaction to Y where measurements could be made with facility in most samples. Where the reaction began at temperatures above 750°C. (see Fig. 15 specimen 208), the measurements were made from the assumed temperature origin; and where measurements could not be made to temperature Y (see Fig. 15 specimen U-1993), the boundary of the area measured was the maximum obtainable. Tabulated below are the theoretical and experimental heats of reaction for the ten monoclinic amphiboles.

FIG. 15
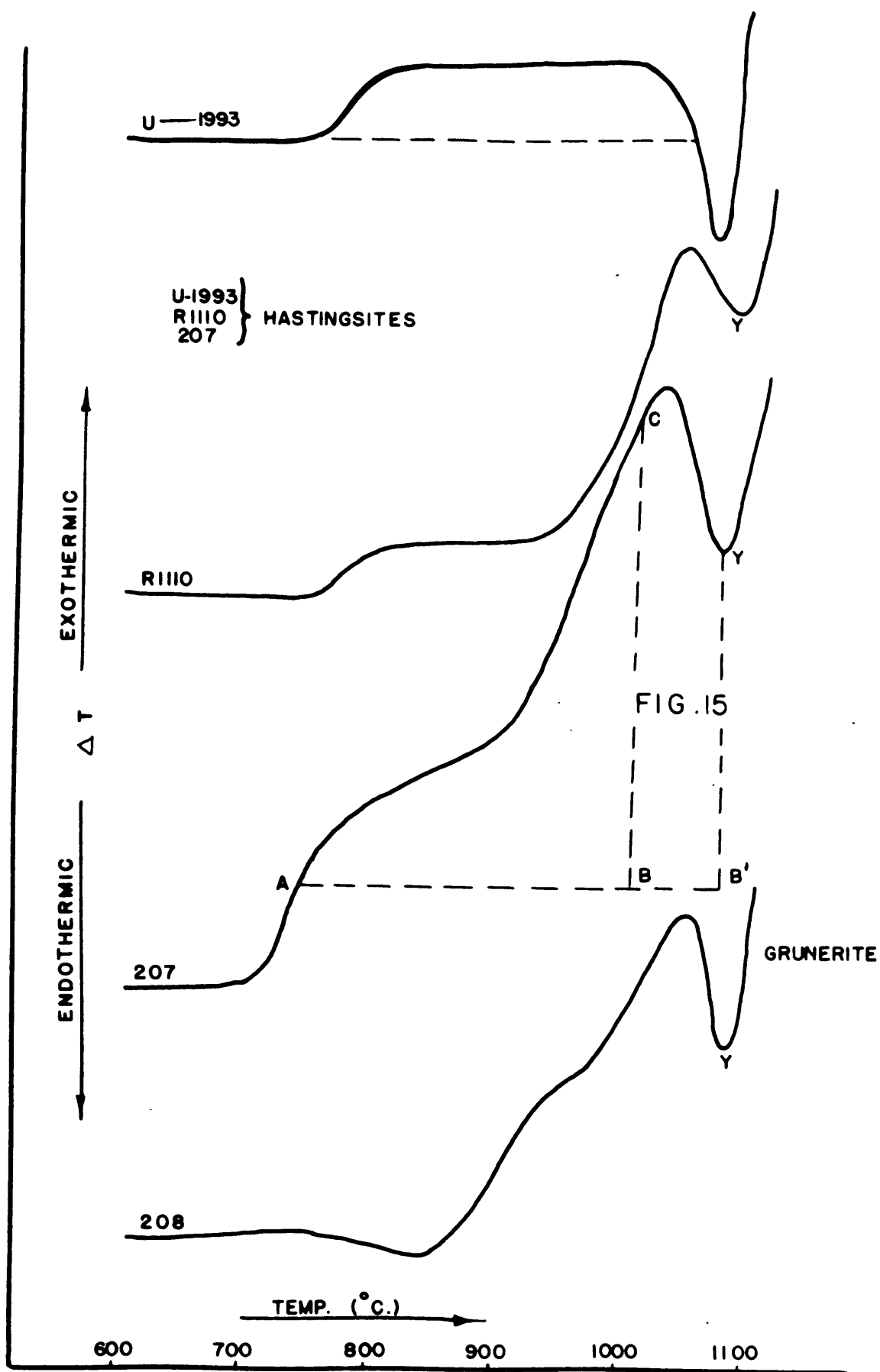
Sample	Name	Theoretical $(-\Delta H)$ Calories	Experimental $(-\Delta H)$ $(750°C-1000°C)$ Calories	Experimental $(-\Delta H)$ $(750°C-Y°C.)$ Calories
U-1993	Hastingsite	1.53	0.42	0.46
R1110	Hastingsite	2.54	0.42	1.07
207	Hastingsite	4.36	0.87	1.65
IH39	Soda Tremolite Glaucophane	0.79	0.31	0.43
IH87	Soda Tremolite Glaucophane	1.13	0.58	0.58
U-184e	Soda Tremolite Glaucophane	1.41	0.38	0.68
U-1954	Soda Tremolite Glaucophane	1.71	0.73	0.76
2017	Actinolite	1.15	0.22	-
208	Grunerite	3.91	0.55	1.11
411	"Arfvedsonite"	1.29	0.65	0.75

The first three samples in the tabulation, the hasting-
sites, should be of the greatest interest, since they are the
common hornblendes upon which most of the previous oxidation
experiments were performed. As expected, the experimental
values for the heats of reaction fell well below the theoretical
values. For the temperature range 750° - 1000°C., these
experimental results are low, as in the anthophyllites, by a
factor of about five, and are somewhat erratic. The experi-
mental heats for the broader temperature span, however, are
considerably closer to the theoretical heats in those specimens
high in FeO (R1110 and 207).
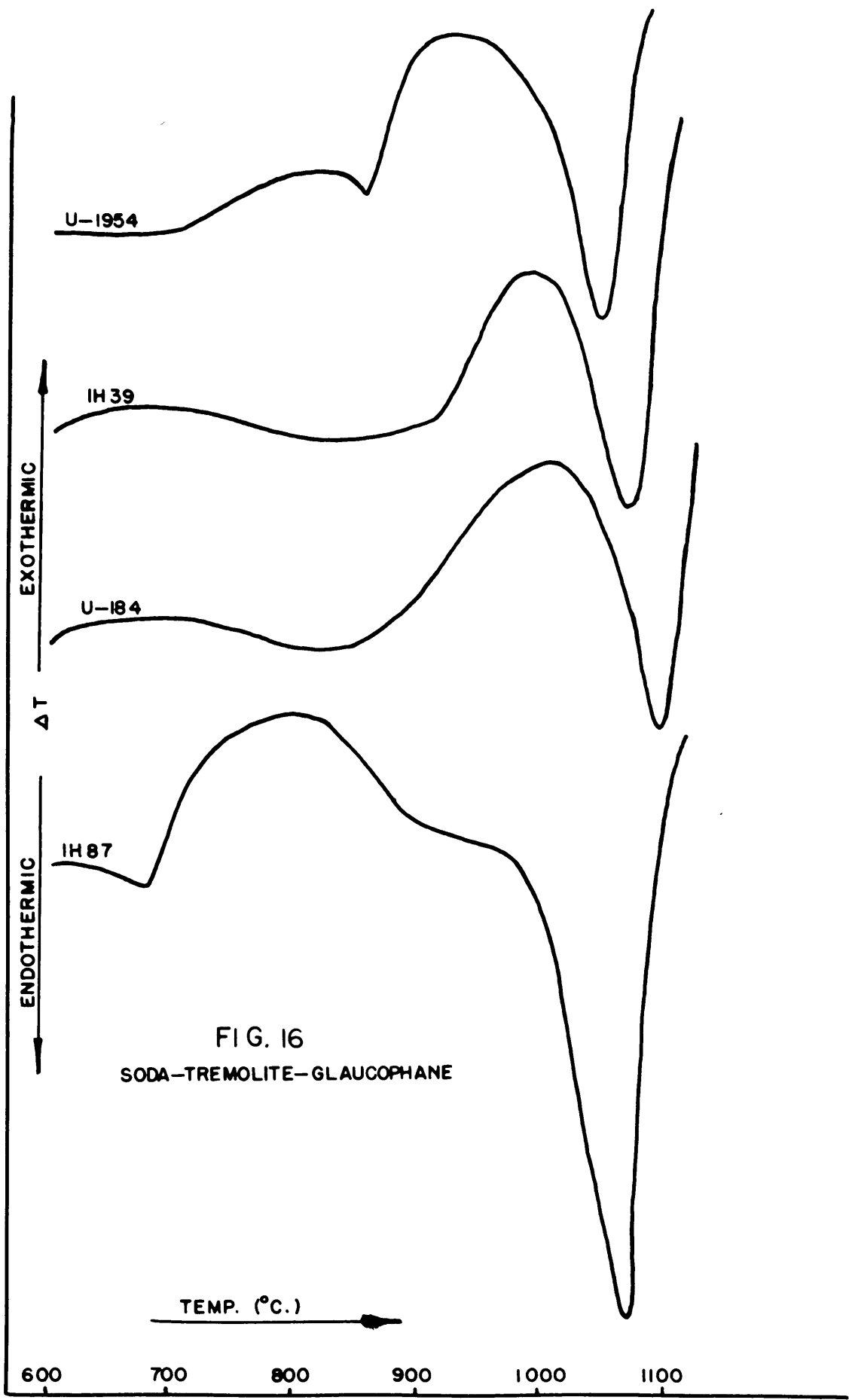
FIG. 16

SODA—TREMOLITE—GLAUCOPHANE

The heats of reaction in the range 750°C - Y°C for the four soda-tremolite-glaucophane specimens gave the best results of the entire investigation. The experimental values were low by a factor of two, which is good qualitative accuracy, but even more significant is the fact that the experimental heats of reaction for the four specimens varied directly with the theoretical determinations. This indicated that differential thermal analysis might be used for the qualitative determination of FeO in amphiboles of this species. In the temperature range 750° - 1000.C, the determination of the experimental heats of reaction for these four species gave fair results except for the irregularly high determination for specimen IH87. Spectrographic examination of this specimen revealed a very high TiO_2 content (6.0%). What effect this composition had on the oxidation of ferrous iron is not explained; nevertheless, it appears to have had some bearing on the thermographic analysis of the specimen (Fig. 16). Of the four thermographic curves for soda-tremolite-glaucophanes this particular specimen displayed the most radical thermographic record. The major exothermic reaction began about 700°C., considerably lower than in the other specimens.

The last three specimens 2017, 208, and 411, were placed together in the tabulation because they represented single members of diverse monoclinic amphiboles.

The experimental results for these three samples were low
and erratic; nevertheless a closer examination of the
results revealed some interesting features. The grunerite
specimen contained the highest FeO content (29.45%) and
its thermographic record gave the lowest comparable energy
change for the oxidation of ferrous iron in the entire
analysis. Its experimental heat of reaction measured over
the short temperature span was low by a factor greater
than 7. On the other hand, specimen 411 (Fig. 17), highest
in Fe_2O_3 content, displayed an experimental energy change
that differed from the theoretical value by a factor less
than 2. Although these results are not at present explained,
one empirical conclusion may be drawn. Ferrous iron content
as determined by differential thermal analysis is most
accurately determined in the soda-rich amphiboles, particu-
larly the glaucophane-arfvedsonite members. By noting that
the experimental heats are low by a factor of about 2 in
these minerals, one may obtain a rapid qualitative analysis
for FeO.

FIG. 17
ARFVEDSONITE
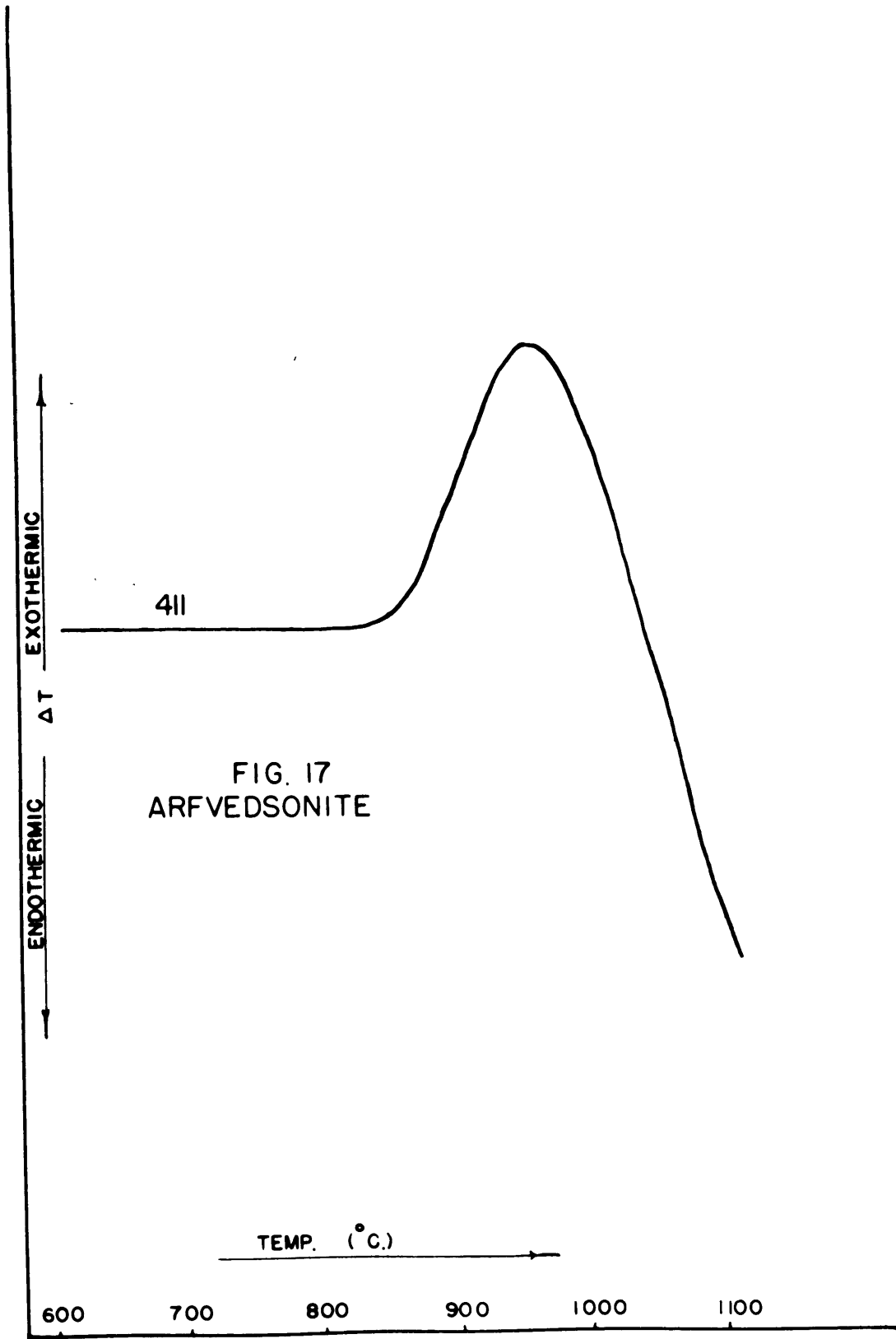
Structural Disintegration of the

Monoclinic Amphiboles

The phenomenon of structural collapse of the mono-
clinic amphiboles was recorded sharply by their thermographic
curves at temperatures between $925 \pm 20.C.$ and $1125 \pm 20°C.$
As in the anthophyllites, this transformation is a solid
state reaction requiring heat absorption (endothermic). The
area XYZ of the thermographic curves was defined as the
reaction area for structural disintegration.

Tremolite:

The determination of the heat of reaction for the
structural collapse of hydroxyl tremolite was the most
accurate calorimetric analysis in this investigation. This
greater accuracy was a direct result of two important factors:
(1) No oxidation reaction interferes, (2) The absence of
alkalis and fluorine eliminates the inaccuraeies which are
imposed by fusion.

The thermographic curves for the tremolites (Fig. 14)
define the origin temperature (X) at $950°C.$, reaction peak
temperature (Y) at $1040°C.$, and completion temperature (Z)
at about $1100°C.$ All these temperatures are $\pm 20.C.$

The thermographic curves for specimen 204 describe
the endothermic reaction.

$$Ca_2Mg_5Si_8O_{22}(OH)_2 + \Delta H = 2CaSiO_3 \cdot 5MgSiO_3 +$$

$SiO_2 + H_2O$ (16) most accurately because its chemical composition comes very close to the theoretical formula for a hydroxyl tremolite. The heat absorbed ($+\Delta H$) in the above reaction was also measured for four other tremolites, with the following results:

Tremolite Specimen	Heat of Reaction ($+\Delta H$) $\pm$ 15% Cal. per Gram	Physical Nature of Specimen at 1100°C.
204	6.4	Unchanged
203	6.2	Unchanged
206	6.35	Unchanged
47863	6.7	Unchanged
202	2.0	Partially Sintered

The most striking feature of the analysis was the consistency of the results with the exception of the analysis for 202, the high alkali-fluoride specimen. The sintering of this specimen resulted in a heat of reaction measurement that was very low in comparison with the others. The reaction which may have taken place in this sample, to describe the somewhat different thermal record, is

$$2\,NaCa_{1.5}Mg_5Si_8O_{22}(F)(OH) \quad (+)\,\Delta H = \begin{array}{l} 3CaSiO_3 \\ 10MgSiO_3 + H_2O + 2NaF \cdot 3SiO_2 \\ \text{diopside-} \\ \text{clinoenst.} \end{array} \quad \text{glass} \quad (17)$$
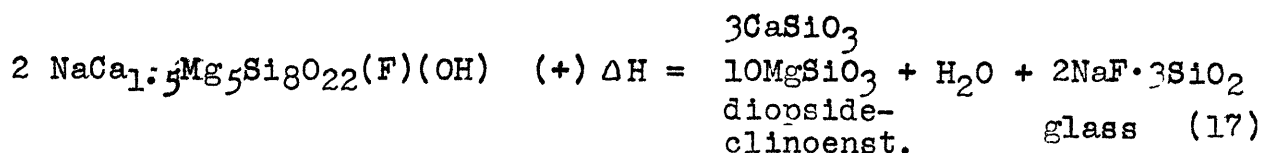
No cristobalite lines were identified from the x-ray powder diffraction patterns. The glass end product of reaction caused extensive scattering of the X-rays which resulted in a diffuse background on the film.

The reaction velocity for structural disintegration indicated an interesting chemical correlation in the tremolites. The slope of XY and the span of XZ were the criteria for these observations. The steepness of the former and the shortness of the latter indicated a relatively rapid reaction velocity. Specimens 204 and 206, showed low reaction velocities and were the samples that contained little or no fluorine. Specimens 203 and 47863 contained 0.27% F and 0.56%F, respectively, and indicated noticeably higher reaction velocities for structural disintegration. The fact that 0.56% F did not introduce any sintering effects was worth consideration. Apparently alkali must be present to react with the fluorine for the formation of glass.

Actinolite and Richterite:

These two species of monoclinic amphiboles are not closely related chemically, as for example are the tremolite-actinolite members. Nevertheless, their thermographic records (Fig. 14, No. 2017 and No. 205) indicated a generally similar character.

Since structural disintegration was determined as beginning about 920°C., the small endothermic peaks at about 900°C., both curves, are the records of some unknown reactions. The heats of reactions for structural collapse of these two samples are shown below:

Specimen	Name	Heat of Reaction (+) ΔH ± 15% Cal. per Gram	Reaction Peak Temperature ± 20°C	Physical Nature of Specimen at 1100°C.
2017	Actinolite	6.2	1020°C.	Not Sintered
205	Richterite	6.85	1020°C.	Partially Sintered

The reaction for specimen 2017, Actinolite, was similar to that for the disintegration of the tremolites, except that the small amounts of Fe and Al present resulted in the formation of the more complex pyroxene, augite.

The reaction products of specimen 205, a manganiferous richterite, were a complex pyroxene with a composition between johannsenite ($CaMnSi_2O_6$) and diopside ($CaMgSi_2O_6$) an alkali fluoride glass, and some water.

The heats of reaction for the structural collapse of both of these minerals came noticeably close to that determined for the tremolites. This is a direct reflection of the close chemical relation between the series tremolite-actinolite-richterite. The reaction peak temperature for structural collapse was about 40°C. lower in these samples as compared

with the tremolites. This indicated that Fe^{++} and Mn^{++}, when found in small concentrations in the more magnesian varieties of amphiboles, hastened the collapse of the structure. Ignoring for the moment any knowledge of the more ferrous varieties, one might reason that the Fe-O and Mn-O bonds are weaker than the Mg-O bonds as a result of the greater ionic volumes of Fe^{++} and Mn^{++}. Continuing this argument, it follows that these bonds are ruptured at a lower temperature and therefore the entire structure disintegrates at a lower energy level.

Fibrous Soda Tremolite:

Thermographic curves for two fibrous varieties of soda-tremolite (16948, U-1994) were included in the investigation to demonstrate the inability of the thermal analyzer to measure accurately the energy changes in fibrous substances. This was directly due to the difficulties encountered in packing these materials about the thermocouple head in the analyzer crucible. The energy changes for structural breakdown in these minerals were indeterminate by the thermal techniques employed in this investigation.

Soda-Tremolite-Glaucophane:

The structural disintegration of specimens whose composition includes portions of the end-members was generally similar to the rupture of the tremolite-richterite samples.

The breakdown products included a pyroxene of the acmite-
augite series, hematite, cristobalite, and water. A
hypothetical reaction for this process is given below:

$$Na_2Mg_2Fe^{++}Fe_2^{+++} Si_8O_{22}(OH)_2 + \frac{1}{4} O_2 + \Delta H = \tag{18}$$

$$
\begin{array}{lll}
2NaFe^{+++}Si_2O_6 & & \\
2MgSiO_3 & + \frac{1}{3} Fe_2O_3 + & 2SiO_2 + H_2O \\
\frac{1}{6}Fe_2O_3 & & \\
\text{polyaugite} & \text{hematite} & \text{cristobalite}
\end{array}
$$
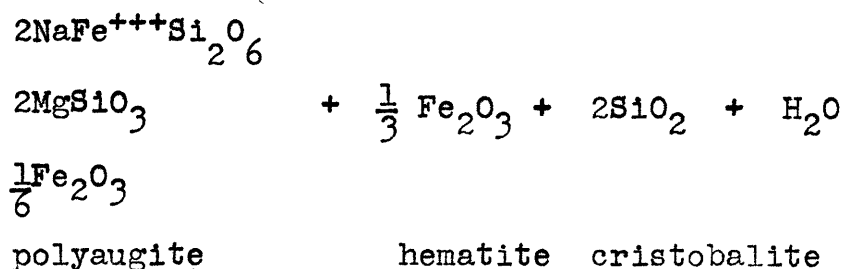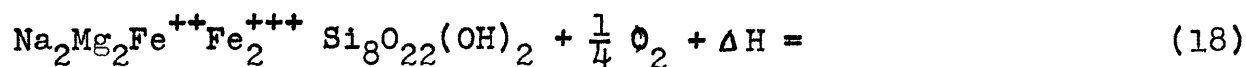
This reaction varies from specimen to specimen depending
upon the chemical composition of each amphibole. Small
amounts of calcium and aluminum in these specimens alter the
reaction only slightly since both are acceptable constituents
of the augite reaction product. Indeed, the ability of the
augite structure to accept small amounts of Al^{+++}, Fe^{+++},
and Ti^{++++} in addition to regular amounts of Ca^{++}, Mg^{++}, Fe^{++},
and Mn^{++} makes it almost impossible for any precise reaction
to be written. Slight differences in the content of the
isomorphous constitutents of the amphibole minerals definitely
alter the proportional amounts of the reaction products.
The presence of fluorine will cause the formation of a glass
and reduce the amount of pyroxene component. In a limiting
case one or more of the reaction products shown above might
not form. An example of this is a glaucophane whose iron

content is so low that all the Fe goes into the pyroxene
reaction product at the expense of the hematite formation.
In any case, the bulk of the disintegration products always
consists of a complex pyroxene of the acmite-augite-clinoen-
statite series while the remaining products described above
form in minor amounts or are absent. The discussion con-
cerning the heats of reaction for the disintegration of these
amphiboles is confined therefore to a loosely defined
reaction in which the major reaction product is a complex
monoclinic pyroxene.

Soda Tremolite-Glaucophane Specimens	Heat of Reaction $(+\Delta H)$ $\pm$ 25% Cal. per Gram	Physical Nature of Specimen at 1100°C.
U-184e	5.24	Fused
IH39	4.68	Fused
U-1954	7.00	Fused
IH-87	10.81	Fused

The temperature peak (Y) for the disintegration
reaction varies between 1050°C - 1110°C. The higher
energy requirement for the structural rupture of certain
samples is probably due to the large amounts of sesquioxides
and Ti^{++++} present. These cations are small and highly
charged and therefore the electrostatic bonds of their cation-
anion linkages require a greater amount of energy for rupture.

The estimated accuracy of the calorimetric measurements
($\pm$ 25%) is lower as a result of the fusion occurring during
the reaction.

Arfvedsonite:

The close genetic relationship between arfvedsonite
and glaucophane was revealed by their thermographic curves.
One might expect a close relationship between their dis-
integration products also, and this too was confirmed. A
soda-rich polyaugite, large amounts of hematite, and a
sodium silicate glass were identified from the fused dis-
integration products. The quality and quantity of these
products reflected the high Na_2O (15.0%) and Fe_2O_3 (21%)
contents of sample 411. Apparently the formation of a very
large quantity of glass resulted in the absorption of an
abnormally large amount of heat since the thermal curve
(Fig. 17) recorded the rapid absorption of heat as high as
1100°C. Although quantitative calorimetric data for the
heat of reaction could be obtained from this thermographic
record, a qualitative estimate would be 10-15 calories per
gram, a value somewhat higher than any of the heats for
glaucophanes.

Pargasite – Hastingsite:

These amphiboles are members of the lime-alkali varieties of hornblendes that are conspicuously high in calcium as well as in aluminum. An interesting breakdown product was identified in addition to those substances already described. Specimen R1110 heated to 1100.C. reacted to form polyaugite, hematite, and flakes of plagioclase. The complex composition of both the amphibole and its reaction products prohibits the writing of a precise expression for the reaction but a general reaction may be expressed as follows:

(Specimen R1110)

Pargasite-Hastingsite (+) ΔH = Polyaugite + Hematite + Plagioclase + Water   (19)
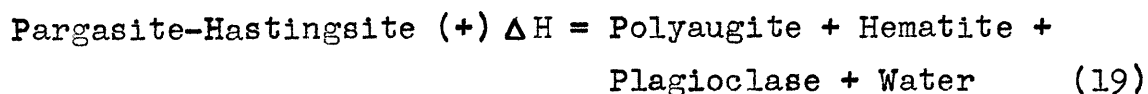
The same specimen heated to 1145°C. reacted to form all the products above plus some olivine and magnetite. This was the first appearance of olivine in the disintegration products of the amphiboles in this investigation. Evidently temperatures greater than 1125°C. are needed for the formation of an olivine disintegration product. The structural disintegration products of U-1993 at 1100°C. were the same as those for R1110. At 1100°C., the reaction products identified from specimen 207 were polyaugite, magnetite, and some glass. The glass formation probably prevented the formation of any plagioclase.

The reaction temperature origin (X) is 1020°C. ± 20°C. and the peak temperature (Y) is 1085°C. ± 20°C. for the pargasite-hastingsite hornblendes. These temperatures lie in the range for structural collapse of the glaucophane specimens. The heats of reaction (+ ΔH) for the structural disintegration of the three specimens are shown below:

Specimen	Heat of Reaction (+) ΔH ± 15% Cal. per Gram	Reaction Peak Temperature + 20°C.	Physical Nature of Specimen at 1100.C.
U-1993	2.83	1085°C.	No Fusion
R1110	0.83	1090°C.	Slightly Sintered
207	3.33	1085.C.	Fused

The heats of reaction for these aluminous hornblendes are of the same order of magnitude as those for the tremolites and glaucophanes but the values are noticeably lower. The aluminous anthophyllites also gave low heats of reaction for the structural disintegration reaction. A possible explanation of these low energy requirements is that Al^{+++} substituting for Si^{++++} makes the chain linkages weaker than pure Si-O bonds. The lower valence and large radius of the Al^{+++} ions supports this explanation.

Structural Changes in Tremolite and Richterite at about 825°C.:

Tremolite:

The thermographic curves of all the tremolite samples reveal a sharp exothermic reaction taking place about 825°C., with a base line shift at the completion of the reaction. The general configuration of the reaction peaks are strikingly similar to thermal curves showing the $\alpha \rightarrow \beta$ quartz inversion; both occur over a narrow range of temperature and indicate a sharp thermal conductivity change at the completion of the reaction. However, the peculiar phenomenon of heat evolution with rise in temperature contradicts the seemingly apparent displacive transformation. The problem therefore is parallel to the one encountered in the investigation of the magnesian anthophyllites. With the exception of a distinct thermal conductivity change beyond the transformation point in the tremolite, both magnesian varieties of amphiboles display a marked parallelism of thermal properties. These are: (1) Apparent irreversibility (thermographically) of the reaction, (2) Apparent non-existence of a high form at 850°C., and (3) A heat of reaction near (-)2.75 calories per gram for the transformation.

Dilatometric tests on specimen 203 revealed a
contraction in the direction of the C-axis at 825°C. that
was not reversible. The experimental results indicated
an approximate c-axis shrinkage of 0.65% as shown below:

Specimen	Temperature °C.	Length (c) (any units)
203	100	45.6
	300	45.6
	500	45.6
	775	45.6
	825	45.3
	775	45.3
	700	45.3
	825	45.3
	900	45.3
	1000	45.3
	1050	45.3

The base line shift in the thermographic curves for the
tremolites at about 900°C. made precise calorimetric
measurements indeterminable. By reversing the sequence
of area measurement an approximate calorimetric deter-
mination was made possible. This was accomplished by
extending the base line at reaction completion to the
lower temperature portion of the curve and employing the
area thus obtained for the energy determination. A

cursory examination of this area (Fig. 14) indicated that it is low by a factor of about one-half, therefore all the values were multiplied by 1.5 in the evaluation of $(-)\Delta H$.

Specimen	Heat Evolved Cal. per Gram
204	2.76
203	2.76
202	2.00
47863	2.50
206	0.75

The slight variations in the energy determinations are no doubt due to the variations in composition from the pure tremolite formula. It should be noted that the energy of transformation for tremolite and magnesian anthophyllite is approximately the same, and that the dilatometric test is not reversible for tremolite.

Richterite:

At about 700°C. richterite (Fig. 14, 205) starts to undergo an exothermic transformation that reaches a maximum about 825°C. This transformation is not rapid and evolves considerably more heat than the corresponding transformation for tremolite. The reaction is thermographically irreversible even if the peak temperature (825°C.) is not exceeded.

Quenching experiments established a structural change in the nature of a crystallographic contraction. X-ray powder diffraction patterns (Fig. 18) revealed a slight increase in the values for Θ, in other words, a decrease in the d spacings. No new lines appeared nor were any of the original lines extinguished in the patterns of specimens quenched at about 825°C. A decrease in the distances between interatomic planes in a crystal results in a volumetric contraction of the crystal structure which can be mathematically evaluated if the values for Δd are known and the various lines indexed. Shinoda[36] derived the equations for the changes in the lattice constants with respect to changes in d for all the crystal systems except monoclinic and triclinic by differentiation of the basic relations for each system. Differentiation of the formula for the monoclinic system

$$d_{hkl} = \cfrac{1}{\sqrt{\cfrac{\dfrac{h^2}{a^2} + \dfrac{l^2}{c^2} - \dfrac{2hl\,\cos\beta}{ac}}{\sin^2\beta} + \dfrac{k^2}{b^2}}}$$

obviously results in a complex and unwieldy expression due to the presence of the radical and the β terms.
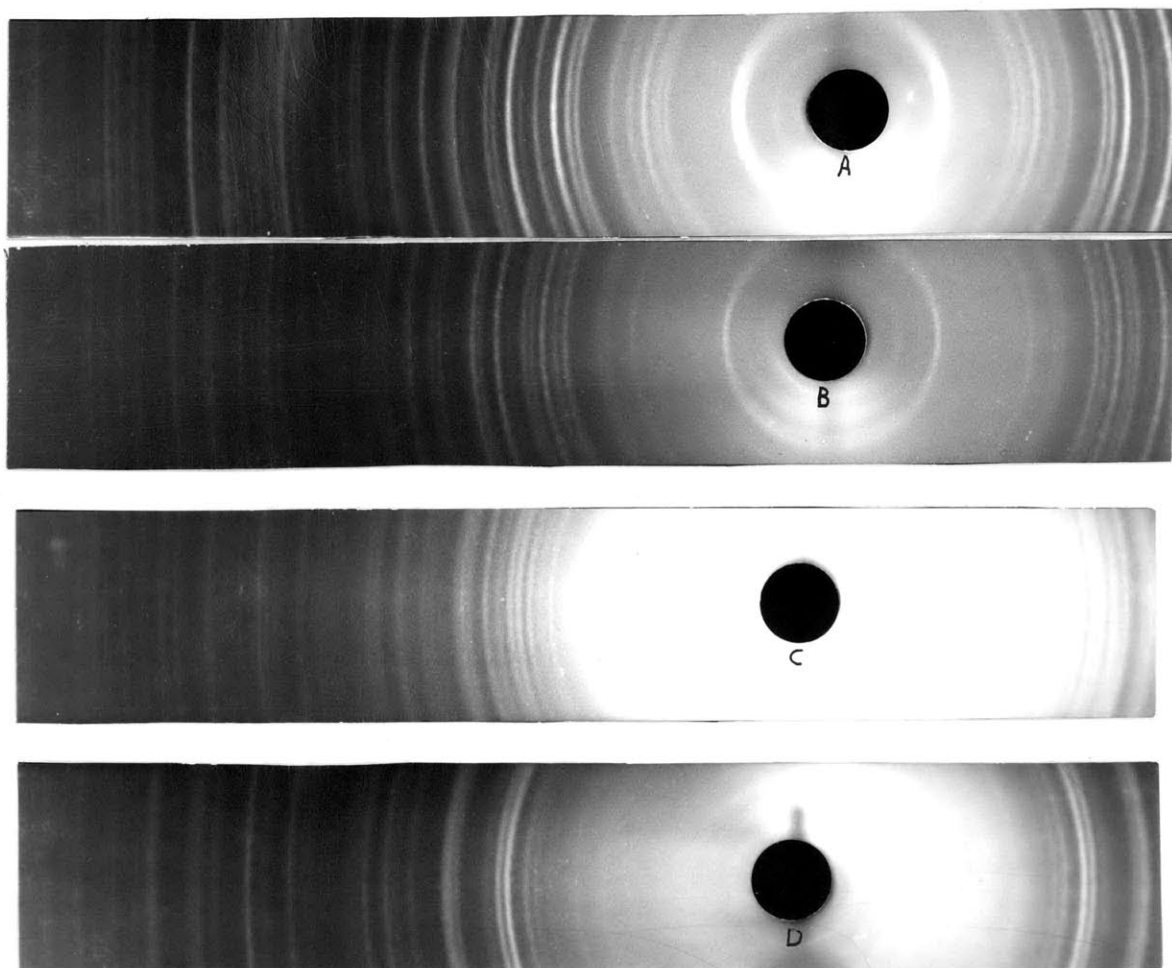
Figure 18

Richterite

X-Ray Powder Photographs, Copper Kα Radiation.

A. 114.6 mm. camera (forward reflections only).

B. Same as A, but quenched from 825°C.
   Note decreased d spacings.

C. Same as A, but quenched from 950°C.
   Diffraction spectra of rupture products begin to appear.

D. Same as A, but quenched from 1050°C.
   Disintegration reaction complete. New diffraction spectra.

Since x-ray powder diffraction patterns do not give a high order of precision, an approximate method was employed in the determination of the changes in the lattice constants of richterite at 825°C. Although there are four constants in the monoclinic crystals, a, b, c, and β, only the changes in the axes were determined. Two assumptions were made in this approximate method:

(1) Since the tables compiled by Struntz[37] do not include the cell constants for richterite, the constants for tremolite were substituted:

a_0 = 9.78 Å, b_0= 17.8 Å, c_0 = 5.26 Å, and β = 106° 2'.

(2) The crystal was assumed to be orthorhombic because is close to 90°.

The last assumption did not introduce any large error into the analysis and permitted the use of Shinoda's equation for the thermal expansion of orthorhombic crystals:

$$\frac{\Delta d}{d} = \frac{1}{\dfrac{h^2}{a^2} + \dfrac{k^2}{b^2} + \dfrac{l^2}{c^2}} \left[\frac{h^2}{a^2}\frac{\Delta a}{a} + \frac{k^2}{b^2}\frac{\Delta b}{b} + \frac{l^2}{c^2}\frac{\Delta c}{c} \right] \quad (20)$$

Using this formula and the assumptions above the following changes were derived:

(hkl)	$d_{700°C.}$	$d_{825°C.}$	Δd	$-\Delta a$	$-\Delta b$	$-\Delta c$
(300)	3.1367	3.1260	0.0107			
(550)	1.6548	1.6489	0.0059	0.033361	0.072548	0.028815
(003)	1.5882	1.5795	0.0087			

a_0	b_0	c_0	a_0 % Expansion	b_0 % Expansion	c_0 % Expansion
9.78	17.8	5.26	-0.33	-0.44	-0.55

The axial contractions are of the same order of magnitude as those for magnesian anthophyllite (0.44%) and tremolite (0.65%). The systematic and random errors of the determination make the accuracy of the analysis $\pm$ 25%. The negative values for Δa, Δb, and Δc indicate contraction rather than expansion.

Becker[38] gives the following expression for the average thermal coefficient of expansion of a solid by the x-ray powder diffraction method:

$$1 + \alpha(t_2 - t_1) = \frac{\sin \frac{\theta_1}{2}}{\sin \frac{\theta_2}{2}} \tag{21}$$

is the average coefficient of linear thermal expansion between temperatures t_1 and t_2, θ_1 is the angle at t_1, and θ_2 is the angle at t_2. The same equation is employed here for the determination of the average thermal coefficient of contraction.

| (hkl) | 700°C. | | $\Delta\frac{\Theta}{2}$ | 825°C. | | $1 + \alpha$ |
	$\frac{\Theta_1}{2}$	$\sin\frac{\Theta_1}{2}$		$\frac{\Theta_2}{2}$	$\sin\frac{\Theta_2}{2}$	$(t_2 - t_1)$
(300)	7°6.4'	0.12398	0°1.5'	7°7.9'	0.12414	0.99871
(550)	13°52.1'	0.23969	0°3'	13°55.1'	0.24054	0.99646
(003)	14.30'	0.25038	0°5.3'	14°35.3'	0.25188	0.99402

Average coefficient of linear thermal contraction is

$$\alpha = \frac{0.99639 - 1.00000}{825 - 700} = 2.8 \times 10^{-5} \text{ per deg. C.}$$

The significance of this coefficient is more apparent when one realizes that the coefficient of linear thermal expansion for most metals is of the order of magnitude of 10^{-5} per degree Centigrade.

Figure 15 (207 and R1110) reveals changing slopes in the thermographic curves in the 750° - 800°C. range. The change is not so pronounced as that for the tremolites, richterite, and magnesian anthophyllites; neverthelss, it offers support for Kozu's dilatometric experiments on common hornblendes.

Fluorine in Monoclinic Amphiboles:

It has been shown repeatedly that fluorine plays an important role in the structural collapse of the amphiboles, both orthorhombic and monoclinic. Fluoriferous specimens

heated to a temperature of 1125°C. and spectrochemically analyzed, revealed no loss of F as in the anthophyllites. As described previously, for those specimens high in Na and F, for example IH39, the x-ray powder diffraction pattern of the structural breakdown products was highly obscured by background effects. These were due to the scattering of the x-rays by the alkali-flurosilicate glass.

The facility for interaction of sodium and fluorine can be demonstrated by an examination of their roles in the amphibole structure. Univalent sodium is in 8-fold coordination with oxygen, forming eight ionic bonds of strength $\frac{1}{8}$. The large size of the Na$^+$ (0.98 Å), and its weak oxygen bonds, indicate that these are the first bonds broken when structural disintegration is initiated. Although fluorine is more strongly bonded (three bonds of $\frac{1}{3}$ strength) to cations in the divalent magnesium position, it is these bonds, as well as the cation-anion bonds of the X and Y elements which are ruptured with the least energy. Fluorine's extremely high electronegativity[39] (4.o) indicates why it immediately combines with the freed sodium to form an NaF glass. Above 1000°C., the melting and sintering effects of these high alkali-fluorine amphiboles is understandable since the melting point of pure sodium fluoride (NaF) is 992.C.

The exact geochemical relations of fluorine in monoclinic amphiboles based on only seventeen analyses could not be determined. Most, if not all, of the specimens analyzed were rather large crystals or aggregates from highly mineralized rocks and could be expected to contain high concentrations of F. Analyses for F in the seventeen samples supported this contention. Below are tabulated the fluorine concentrations in varieties of monoclinic amphiboles investigated here.

Specimen	Name	%F	Group Average
204	Tremolite	-	
203	Tremolite	0.27	
47863	Tremolite	0.56	
206	Tremolite	0,11	0.40
202	Tremolite	1.35	
2017	Actinolite	0.11	
205	Richterite	0.37	
16948	Soda Tremolite	1.30	1.22
U-1994	Soda Tremolite	2. +	
IH39	Soda Tremolite Glaucophane	2.14	
IH87	Soda Tremolite Glaucophane	0.17	1.18
U-184e	Soda Tremolite Glaucophane	2. +	
U-1954	Soda Tremolite Glaucophane	0.41	

Specimen	Name	% F	Group Average
U-1993	Hastingsite	–	
R 1110	Hastingsite	0.12	0.16
207	Hastingsite	0.36	
411	Arfvedsonite	0.14	0.14

Average F in 17 samples = 0.67%   Accuracy ± 10%

The very high fluorine concentration in the soda
rich amphiboles is not to be construed as a general
characteristic.   In addition, the low average fluorine
content (0.16%) in the hastingsite members is not very
significant.   It is more likely that the analyses of the
tremolite-actinolite group come very close to displaying
the trend of fluorine concentration in monoclinic amphiboles.
The average content in 6 specimens (0.40% F) is probably
higher than the concentration that might be found in the
hornblendes in an average granite.   An estimate of the
average fluorine content of amphiboles in normal granite
is 0.25-0.35% F.

Some Minor Element Determinations:

A spectrochemical analysis for minor elements,
parallel to that for the anthophyllites, was made on sixteen

specimens of monoclinic amphiboles. As before, Mn, Ti, Li, Na, and F were defined as sub-major elements, while Co, Ni, Cr, and V were designated as minor constituents.

Actually Na is a major element in most monoclinic amphiboles, but, since its range of concentration was found to vary between 0 and 15% Na_2O, it was included in the minor element analyses. Little can be stated concerning the relations of Na, beside noting that sample 411 contained the extremely high Na_2O content of 15.0%. The theoretical Na_2O content of a pure eckermannite is 11.6%, and this value is the maximum theoretical Na_2O content for all the amphiboles. In all probability, the analysis of 15.0% is too high and is more likely closer to 12%. Sodium followed the Sundius classification[35] in the remaining suite of specimens.

The alkali element lithium showed no preference for any particular amphibole group and except for the lithium amphibole, holmquistite, the average was about 0.05% Li in most members.

In the tremolite-richterite sequence, TiO_2 was found in average amounts of 0.15%. Specimens containing the glaucophane and arfvedsonite end-members averaged about 0.30% TiO_2, and hastingsite samples contained higher concentrations that averaged about 1.4%. The very high TiO_2 and Fe_2O_3 contents in specimen IH87 and the correspondingly low F content indicated that this specimen may be one of the more anhydrous

varieties of amphiboles which Warren[34] postulated for sesquioxide-rich minerals. The common titanium-iron relationship was demonstrated throughout the analysis.

Vanadium was absent or very low in the tremolites. In all the remaining specimens, however, V content remained quite constant (0.20%) and independent of the Fe^{+++}, Al^{+++}, and Ti^{++++} concentrations in these minerals. V^{++++} usually replaces these cations in igneous rocks, but this relation apparently does not apply to the amphibole minerals.

The transition elements, Ni and Co, did not show the preferential concentration in magnesium rich monoclinic amphiboles, that was noted in magnesium rich anthophyllites. On the contrary, both metals were found almost completely lacking in the tremolites. Nor did Ni^{++} indicate a preferential following of Fe^{++}, for it was found in equal magnitudes in soda tremolites as well as hastingsites.

The replacement of octahedrally coordinated Al^{+++} and Fe^{+++} by Cr^{+++} is demonstrated by the higher chromium analyses in hastingsites and glaucophanes. An exception to this statement is the fact that the two highest analyses for Cr, 0.3% and 0.2%, were determined in actinolite and soda-tremolite respectively. Generally, however, the diadochic replacement for Fe^{+++} and Al^{+++} was upheld.

Mn^{++} plays a unique role as a minor element for it may occupy either the X or Y positions in 8-fold or 6-fold coordination. This means a greater freedom for sites in the monoclinic amphiboles for which Mn^{++} can compete, and this should be reflected by comparable concentrations in all the members of this group. The analyses for MnO confirmed this observation, as all but one specimen contained at least 0.03% MnO. The average of 17 samples was 0.46% MnO, which is too high for a general average. The manganiferous richerite sample (205) contained 2.40% MnO and raised the average above normal. An estimate for the average MnO content in monoclinic amphiboles is close to 0.30%.

A special note of interest is the minor element analysis for specimen 2017, an actinolite. This mineral contained 0.3% Ni, 0.3% cr, and 0.008% Co, the highest concentrations for these elements in the entire analysis. The magnesian anthophyllites rich in these constituents also indicated the same relationship between Ni, Cr, and Co, namely that the Ni and Cr content is 20 to 40 times higher than the Co content. All of these high concentrations, it was noted, were confined to magnesian amphiboles, ortho-rhombic and monoclinic and it is recalled that these are metamorphic minerals.

The high concentrations of Ni, Cr, and Co in magnesium-rich metamorphic amphiboles were the outstanding characteristics of the minor element determinations. Apparently the metamorphic mineral assemblage favors the inclusion of these minor elements in the magnesium-rich amphiboles. Also of interest was the observation that any amphibole, igneous or metamorphic, high in one or two minor elements, was generally higher in all of the minor elements. This indicated the relative importance of the availability of the elements during mineral crystallization. The characteristics of ionic radius, type of bonding, and coordination number are all essential to the evaluation of a minor element analysis, but it is felt that the importance of the availability of the elements often may be overlooked.

SUMMARY

Methods of Analysis:

Orthorhombic and monoclinic amphiboles were studied
by thermal, spectrochemical, and x-ray methods. The
thermal method of investigation was a technique of differ-
ential thermal analysis that permitted micro-calorimetric
measurements to be made. The measurements were made
possible by a calibration of the analyzer which resulted
in a linear relation between the energy changes and the
thermographic responses (areas under the curves). The
success of this type of analysis was largely dependent
on these factors:

(1) A heat source made up of a low-inertia
radiation-type furnace.

(2) The employment of high heating rates ($30°C.$
per minute) to amplify the reaction peaks.

(3) The use of minute samples for analysis in
order to eliminate base-line deviations.

It was shown that low heating rates ($10°C.$ per minute)
diminished the thermographic response considerably and
an empirical relation was established between the heating
rate and the thermographic response. Sixty milligrams
was found to be the optimum mass for the calorimetric
determinations of the amphiboles. The differential

thermal analyses were made at a heating rate of 30°C.
per minute, in a furnace evacuated to 1 mm. Hg. The
temperature range of analysis was 600°C-1125°C.

Where chemical analyses were not available, specimens
were spectrochemically analyzed for the major elements. In
addition, a complete spectrochemical analysis for fluorine,
the alkali metals, and the minor elements was made. Ordinary
x-ray powder diffraction methods were employed to detect
structural transformations indicated by the thermographic
curves.

Anthophyllites

The investigation of seven anthophyllite specimens
included these topics: (1) The role of hydroxyl and fluorine,
(2) The oxidation of ferrous iron, (3) Structural disin-
tegration phenomena, (4) Structural transformations at 800°C.-
825°C., and (5) Minor element determinations.

Role of Hydroxyl and Fluorine:

The general formula $X_7Y_8O_{22}(OH,F)_2$ for anthophyllites
shows two (OH+F) groups per mole. The theoretical weight
per cent of (H_2O+F) ranges between 1.95 and 2.2 in these
minerals, but most chemical analyses for these components
fall short of this theoretical range. The reasons for these
low analyses are: (1) Chemical analyses are difficult in

these low ranges, (2) Omission of, or poor analyses for
fluorine, and (3) Possible weight gain by oxidation.

The expulsion of hydroxyl groups as H_2O begins
about 800°C. and continues to approximately 975°C. where
the entire structure starts to disintegrate. The ex-
pulsion of hydroxyl groups was examined as a weight loss
determination by the dynamic method of heating to a
desired temperature, immediately cooling in a dessicator,
and weighing. The dehydration and disintegration reactions
develop in the 975°C. range. Fluorine is not removed
from the structure at temperatures up to 1125°C., but
remains in the structural disintegration products as
an alkali glass that speeds the reaction velocity of the
rupture transformation.

Weight loss determinations and spectrochemical
fluorine analyses indicated that the theoretical analysis
for (H_2O + F) can be substantiated by these experimental
methods. Anthophyllites containing less than 15% FeO
showed no weight gain by oxidation because sufficient
structural oxygen is available from the dehydration process
to convert Fe^{++} to Fe^{+++}.

Oxidation of Ferrous Iron:

The oxidation of ferrous iron occurs simultaneously
with the dehydration process beginning about 800°C. This
oxidation reaction is exothermic and is graphically repre-

sented by the peaks of the thermographic curves in the
temperature range 800°C.-1000°C. The theoretical heats
of reaction were calculated and the experimental heats
of heats of reaction were measured from the areas under
the thermographic curves. Experimental results were low
by a factor of 5. Low experimental results were recorded
also from the oxidation of magnetite and olivine samples
used for calibration.

It was concluded that three factors contributed
to these low determinations: (1) Small energy changes
(2-5 cal. per gram), (2) Large sample size, and (3) Large
temperature span (200°C. or greater) over which the
reaction takes place. It was also predicted that energy
changes in other silicates which occur under these
circumstances will also give low determinations.

Disintegration of the Anthophyllite Structure:

At approximately 1020°C., the magnesian anthophyllites
disrupt in the solid state according to the reaction

$$Mg_7Si_8O_{22}(OH)_2 + \Delta H = 7MgSiO_3 = SiO_2 + H_2O$$

Anthophyllite   Enstatite   Crist.
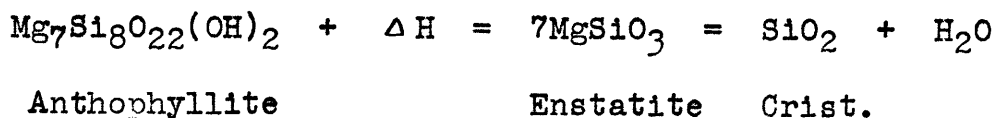
where $(+\Delta H)$ varies between 1.50 and 4.50 calories per
gram depending upon the amount of FeO present.

Ferrous anthophyllites disintegrate in the same
temperature range but the reaction is more complex as
a result of the variable chemical composition. The
products of reaction are hypersthene, cristobalite,
water, and, in the presence of alkalis and fluorine,
a glass. In four specimens, the heat of reaction ($+ \Delta H$)
varied between 0.33 and 2.66 calories per gram. The
reaction is spontaneous at the critical temperature and
the formation of an alkali fluoride glass acts as a
catalyst so that only a small amount of heat is absorbed.
The smallest energy requirements for structural dis-
integration were found in samples containing high
concentrations of Al^{+++} in the Si-O chains.

Structural Changes in Magnesian Anthophyllites at 830°C.:

The thermographic curves recorded a major exothermic
reaction in the 800°C.-850°C. region for magnesian antho-
phyllites. Quenching experiments failed to reveal any
structural transformations that might be identified by
ordinary x-ray powder diffraction methods. The reaction
was irreversible thermographically, possibly as a result
of the rupturing of a few bonds in the initial stages
of structural disintegration.

Dilatometric tests indicated a reversible contraction
in the x-axis direction when the temperature 830°C. was not

exceeded. The shrinkage was 0.44% and the heat evolved in the transformation was between 2.50 and 2.75 calories per gram.

The presence of 8.71% FeO did not interfere with the transformation and it was indicated that the lack of Al_2O_3 may play an even more important role in the transformation. However, further investigation of the phenomenon is necessary before any substantial conclusions can be drawn.

Some Minor Element Determinations:

Spectrochemical analyses for minor elements in seven anthophyllite specimens indicated a major division between magnesian and ferrous varieties.

Li, Na, Ti, and V concentrate in the ferrous anthophyllites as expected. All three magnesian samples contained no less than 0.1% Ni. Cobalt also followed magnesium, but not in such high concentrations. Two magnesian varieties contained no less than 0.2% Cr, and since this relation to magnesium is not common, it was suggested that it might reflect a lower temperature of formation for the magnesian varieties. Mn^{++} showed a preferential concentration in the magnesian specimens despite its large ionic radius which is close to that of Fe^{++}.

Monoclinic Amphiboles

A selected suite of monoclinic amphiboles was
thermochemically analyzed by the same techniques used
in the anthophyllite investigation. The varieties
analyzed included tremolite, actinolite, richterite,
soda-tremolite-glaucophane, arfvedsonite, pargasite-
hastingsite, and grunerite.

Role of Hydroxyl and Fluorine:

Chemical analyses for the $(Oh,F)_2$ group are low
for the same reasons shown in the anthophyllite investi-
gation. Dehydration experiments by the dynamic method
coupled with spectrochemical analyses for fluorine
indicated a full complement of $(H_2O + F)$ within experi-
mental accuracy. The expulsion of hydroxyl groups as H_2O
occurs in the $900°C.-1100°C.$ range and is simultaneous
with the structural disintegration of the mineral framework.
Fluorine remains in the disintegration products of the
amphiboles as an alkali glass that obscures the x-ray
powder diffraction pattern of the breakdown products.
The formation of this glass speeds the reaction velocity
for structural disintegration.

The average F in seventeen samples was 0.67%. The
range of values for this constituent was between 0-2.14%,
diverse end-members containing all ranges. It was estimated
that the amphiboles in an average granite would contain
0.25 - 0.35% F.

Oxidation of Ferrous Iron:

The reaction $2FeO + \frac{1}{2} O_2 = Fe_2O_3$ takes place in
the temperature range 750 C.$^{\circ}$- 1000°C. Theoretical
values for the heat evolved in this reaction were
calculated for the ferrous species. Experimental
determinations for this reaction were low by a maximum
factor of seven. The glaucophane-arfvedsonite specimens
gave experimental determinations which were low by a
factor of two. These particular varieties of amphiboles
gave the best experimental results for this determination
and it was demonstrated that qualitative determinations
for FeO can be made by noting that the experimental
results are low by a factor of two.

Structural Disintegration of Some Monoclinic Amphiboles:

The thermographic curves recorded a clearly defined
endothermic reaction in the temperature range 925°C. - 1125°C.
that was identified by x-ray methods. The reaction is the
collapse of the amphibole structure in the solid state to
form: (1) monoclinic pyroxene, (2) cristobalite, (3) water,
(4) plagioclase, (5) hematite, (6) olivine, (7) magnetite,
and (8) glass. The quantity of heat absorbed by most
specimens when they dissociate is approximately six calories
per gram.

Hydroxyl tremolite breaks down at 1040°C. according to the reaction:

$$Ca_2Mg_5Si_8O_{22}(OH)_2 + \Delta H = 2CaSiO_3 \cdot 5MgSiO_3 + SiO_2 + H_2O$$

Tremolite   Diops.-clinoenst. Crist.

where $(+ \Delta H)$ is about 6.4 calories per gram. The reaction velocity for structural disintegration of fluoriferous tremolites was noticeably higher than that for hydroxyl varieties.

Actinolite breaks down at 1020°C. to give augite, cristobalite, and water. The heat absorbed in this reaction is 6.2 calories per gram.

A richterite containing manganese and fluorine collapsed at 1020°C. to form a pyroxene with a composition between johannsenite and diopside, an alkali fluoride glass, and water. The determination for the heat absorbed in this reaction is 6.85 calories per gram.

Soda-tremolite-glaucophane disintegrates at about 1050°C. to form polyaugite, hematite, cristobalite, glass, and water. The reaction is poorly defined as a result of the variable composition of the amphiboles. The major decomposition product is polyaugite; the other constituents form in small amounts or may be absent. The average heat absorbed in the disintegration reaction of four specimens was 6.9 calories per gram.

Pargasite-Hastingsite amphiboles disintegrate at 1080°C., and higher to form polyaugite, hematite, plagioclase, olivine, magnetite, water, and glass. Olivine and magnetite did not appear until the specimen was heated to 1125°C. Glass formation in fluoriferous varieties prevented the formation of plagioclase. The average quantity of heat absorbed in the dissociation of three specimens was 2.33 calories per gram. The smaller quantity of heat needed to disrupt the structure was attributed to weaker Al-O chain linkages.

Structural Changes in Tremolite and Richterite at 825°C.

The thermographic curves for tremolite revealed an exothermic reaction at about 825°C. that was thermographically irreversible. Approximately 2.75 calories per gram are evolved over a short span of temperature. X-ray diffraction patterns revealed no structural transformation in specimens quenched from 825°C. but dilatometric tests showed an irreversible c-axis shrinkage of about 0.65%.

Richterite undergoes an irreversible transformation that evolves heat at about 825°C. Specimens quenched from 825°C. revealed a crystallographic contraction as shown by decreased d spacings. By an approximate method, the per cent contractions in the a_o, b_o, and c_o directions were determined. These contractions are 0.33% a_o, 0.44% b_o, and 0.55% c_o. The order of magnitude of these changes

follows those for tremolite and magnesian anthophyllite. The average coefficient of linear thermal contraction is 2.8×10^{-5} per degree centigrade. This coefficient is large compared with the coefficients of linear thermal expansion for most metals which are of the order of 10^{-5} per degree centigrade.

Some Minor Element Determinations:

Sixteen specimens were spectrochemically analyzed for Mn, Ti, Li, Na, F, Co, Ni, Cr, and V. An actinolite specimen gave an analysis of 0.3% Ni, 0.3% Cr, and 0.008% Co. the highest concentration for these elements in the entire investigation.

Sodium followed the Sundius classification and varied between 0 and 12%. Li averaged about 0.05% in most members and showed no preference for any particular amphibole group.

The common titanium-iron relationship was demonstrated in the analysis with hastingsite members containing the highest concentrations. TiO_2 averaged about 0.30% in sixteen specimens. Vanadium was low or absent in the tremolites but averaged about 0.20% in all other members. Nickel and cobalt showed no preferential concentration in magnesium members and were almost completely lacking in the tremolites. The diadochic replacement of Cr^{+++} for Al^{+++} and Fe^{+++} was generally maintained.

All but one specimen contained at least 0.03% MnO and the average content for sixteen specimens was near 0.30%.

It was noted also, that any specimen high in one or two of the minor elements was usually high in all the minor elements. This was interpreted as a direct reflection of element availability during mineral crystallization.

SUGGESTIONS FOR FUTURE INVESTIGATION

To obtain more complete understanding of the thermal nature of the amphiboles it is suggested that edenite and tschermakite end-members be examined by the methods used in this investigation. Further study of the volumetric transformations of magnesian anthophyllites, tremolites, and richterites by high temperature x-ray methods might prove fruitful. In addition, if good single crystals of these compositions can be obtained, more precise dilatometric measurements could be made.

Additional uses of the thermal apparatus described in this investigation are numerous. Differential thermal analyses of many mineral species would undoubtedly reveal new and interesting problems for investigation. Calorimetric measurements at elevated temperatures are readily obtainable with the sensitive thermal apparatus used in the investigation and it is recommended that a precise study of hitherto undetermined physical and chemical transformations be undertaken.

Table VII

Summary of

Thermographic Curves

Specimens	Exothermic Reactions	Endothermic Reactions	Fig.	Page
Magnesian Anthophyllites	825°C. reversible cryst. contraction	1020°C. Structural Disintegration	12	40
Ferrous Anthophyllites	750°C.-1000°C. oxidation	1020°C. Same as above	11	37
Tremolites	825°C. irrevers. cryst. contraction	1050°C. Same as above	14	66
Actinolite	750°C.-1000°C. oxidation	1020°C. Same as above	14	66
Richterite	825°C. irrevers. cryst. contraction	1020°C. Same as above	14	66
Soda-Tremolite Glaucophanes	750°C.-1000°C. oxidation	1050°C. Same as above	16	71
Arfvedsonite	700°C.-1000°C. oxidation	1000°C. Same as above	17	74
Pargasite-Hastingsites	750°C.-1000°C. oxidation possible inversion	1080°C. Same as above	15	69
Grunerite	750°C.-1000°C. oxidation	1080°C. Same as above	15	69
Magnetite	330°C. oxidation	520°C. Inversion to Hematite	13	42
Olivine	700°C.-1100°C. oxidation		13	42

TABLE V – CHEMICAL ANALYSES– MONOCL. AMPHIBOLES
WT. PER CENT

Specimen	Name	SiO_2	Al_2O_3	TiO_2	Fe_2O_3	MgO	FeO	MnO	Na_2O	CaO	K_2O	H_2O	F	Total
204	Trem.	55.89	0.10			24.78			0.12	13.95	0.10	2.31	none	99.95
203	Hex.		0.13	0.08		24.8		0.26		13.7			0.27	
47863	Trem.			0.05			1.5						0.56	
202	Trem.			0.18				0.03	0.83				1.35	
206	Trem.			tr				none	<0.35				0.11	
205	Richt.	57.74	0.37	tr	0.29	23.67	tr	2.40	3.14	9.01	0.64	2.39	0.37	99.86
2017	Act.			tr.	2.0	22.5	4.3	0.19	<0.35	13.2			0.11	
16948	Na-Trem.	56.74	0.71	0.28	4.71	21.95	0.87	0.07	5.15	6.05	1.80	0.87	1.30	100.91
U-1994	Na-Trem.	56.00	0.30	0.26	3.91	20.37	2.44	0.55	5.39	5.08	3.01	2.40	none	99.71
U-1954	Tr-Glauc	52.14	4.03	0.47	6.71	15.52	6.40	0.33	7.31	4.49	0.76	1.60	0.41	100.20
IH39	Tr-Glauc	54.30	2.02	0.04	4.32	17.71	2.96	0.52	7.80	3.30	2.10	0.61	2.14	100.95
U-184e	Tr-Glauc	52.28	4.34	0.57	4.32	18.14	5.30	0.26	5.56	6.74	2.18	0.15	n.d.	99.86
IH87	Tr-Glauc	52.94	3.30	1.32	9.87	15.02	4.24	0.15	7.01	3.98	0.48	1.24	0.78	100.45
U-1993	Hastin.	40.18	14.26	1.79	4.73	14.37	5.76	0.22	2.22	5.76	1.86	0.60	0.79	100.19
R1110	Hastin.	43.60	11.33	2.09	4.0	12.41	9.88	0.19	1.38	12.03	1.34	1.63		99.95
207	Hastin.			0.37			16.42	0.52	1.87				0.36	
411	Arfved.		1.95		20.25	3.55	4.85			2.50			0.14	
412	Holmq.	59.58	7.19	0.02	9.35	11.66	4.88	0.41	0.50	0.06	0.27	2.23	0.21	99.92
208	Grun.	52.22	0.58		0.42	12.04	29.45	3.21	Li 1.64 tr	-	-	2.12	-	100.04

ANALYST	TYPE OF ANALYSIS	REF.
E.T.Allen and J.K.Clement }	Chemical	(9)
Author	Spectrochem.	
Author	Spectrochem.	
Author	Spectrochem.	
Author	Spectrochem.	
A.Bygdén	Chemical	(40)
Author	Spectrochem.	
F.Gonyer	Chemical	(43)
F.Gonyer	Chemical	(43)
F.Gonyer	Chemical	(43)
F.Gonyer	Chemical	(43)
F.Gonyer	Chemical	(43)
F.Gonyer	Chemical	(43)
F.Gonyer	Chemical	(43)
A.Buddington / F.Gonyer	Chemical / Chemical	
Author	Spectrochem.	
Author	Spectrochem.	
A.Bygdén	Chemical	(42)
A.Bygdén	Chemical	(41)

Name Code

Trem.   = Tremolite
Hex.   = Tremolite (var.)
Richt. = Richterite
Act.   = Actinolite
Na-Trem. = Soda Tremolite
Tr-Glauc = Soda-Tremolite-Glauco-
          phane
Hastin. = Hastingsite
Arfved. = Arfvedsonite
Holmq. = Holmquistite
Grun.   = Grunerite

TABLE VI — MINOR ELEMENTS — MONOCLINIC AMPHIBOLES
WT. PER CENT

Specimen	Name	TiO$_2$	MnO	Na$_2$O	Li	Co	Ni	Cr	V	F
203	Hexagonite	0.08	0.26	<0.35	0.06	-	0.0033	0.01	tr	0.27
47363	Tremolite	0.05	1.50	<0.35	0.05	-	tr	0.0001	0.009	0.56
202	Tremolite	0.18	0.03	0.33	0.045	-	-	0.001	tr	1.35
206	Tremolite	tr	-	<0.35	0.006	-	-	0.0001	-	0.11
205	Richterite	0.15	2.40	5.0	0.07	-	0.0051	0.001	0.021	0.37
2017	Actinolite	tr	0.19	<0.35	0.009	0.008	0.3	0.3	0.0098	0.11
16948	Soda Tremolite	0.28	0.10	5.0	0.10	0.0025	0.0039	0.2	0.025	1.30
U-1994	Soda Tremolite	0.26	0.52	5.0	0.06	tr	0.0017	0.0015	0.021	2 +
U-1954	Soda-Tremolite-Glaucophane	0.30	0.40	7.5	0.02	0.003	0.0033	0.002	0.022	0.41
IH39	Soda-Tremolite-Glaucophane	0.20	0.52	7.5	0.06	tr	0.0019	0.002	0.02	2 +
U-184e	Soda-Tremolite-Glaucophane	0.40	0.30	5.0	0.12	0.0025	0.0028	0.0028	0.021	2 +
IH37	Soda-Tremolite-Glaucophane	6.0	0.20	7.0	0.03	tr	tr	0.03	0.045	0.17
U-1993	Hastingsite	1.30	0.25	0.87	0.006	0.0054	0.004	0.0054	0.023	tr
R1110	Hastingsite	2.0	0.13	1.41	0.012	0.003	0.0043	0.0068	0.027	0.12
207	Hastingsite	0.37	0.52	1.37	0.06	0.003	0.0031	0.001	0.019	0.36
411	Arfvedsonite	0.30	0.13	15.0	0.06	0.0031	0.0027	-	0.013	0.14
412	Holmquistite	tr	0.40	0.35	1.64	tr	tr	tr	tr	0.21

REMARKS

Ag. absent in most specimens.

Cu. present in almost all specimens in varying amounts.

No. 206 high in Cu.

No. 202 high in Ag

No. 205 high in Ag., some Pb.

ACKNOWLEDGEMENTS

BIBLIOGRAPHY

(1)   Norton, F. H.: "Critical Study of the Differential
      Thermal Method for the Identification of
      the Clay Minerals", J. Am. Cer. Soc.,
      vol. 22, pp. 54-63, 1939.

(2)   Berkelhammer, L. H.: "Differential Thermal Analysis
      of Quartz", Bur. of Mines, R.I. 3763, 1944.

(3)   Speil, S.: "Applications of Thermal Analysis to Clays
      and Aluminous Materials", Bur. of Mines,
      R.I. 3764, 1944.

(4)   Cohn, W. H.:   "The Problem of Heat Economy in the
      Ceramic Industry", J. Am. Cer. Soc.,
      Vol. 7, pp. 475-488, 1924.

(5)   Macgee, A. E.: "The Heat Required to Fire Ceramic
      Bodies", J. Am. Cer. Soc., vol. 9, pp.
      206-247, 1926.

(6)   Shorter, A. J.: "The Measurement of Heat Required
      in Firing Clays", Trans. Brit. Cer. Soc.,
      vol. 47, pp. 1-22, 1948.

(7)   Whitehead, W. L., and Breger, I. A.: "Vacuum
      Differential Thermal Analysis", Science,
      vol. 111, pp. 279-281, 1950.

(7a) Smyth, F. H., and Adams, L.H.: "The System Calcium
      Oxide-Carbon Dioxide", Jour. Am. Chem. Soc.,
      vol. 45, pp. 1167-1184, 1923.

(8)   Ingersoll, L. R., Zobel, O. J., and Ingersoll, A.C.:
      Heat Conduction with Engineering and
      Geological Applications, McGraw-Hill, N.Y.,
      1948.

(9)   Posnjak, E., and Bowen, N. L.: "The Role of Water in
      Tremolite", Am. J. Sci., vol. 22, pp. 203-214,
      1931.

(10) Faust, C. T.: "Thermal Analysis Studies on Carbonates,
      I. Aragonite and Calcite", Am. Min., vol. 35,
      pp. 207-224, 1950.

(11) Beck, C. W.: "An Amplifier for Differential Thermal
Analysis", Am. Min., vol. 35, pp. 508-524,
1950.

(12) Warren, B. E., and Modell, D.I.:   "The Structure of
Anthophyllite, $H_2Mg_7(SiO_3)_8$", Zeit. für.
Krist., vol. 75, pp. 161-178, 1930.

(13) Rabbitt, J. C.: "A New Study of the Anthophyllite
Series", Am. Min., vol. 33, pp. 263-298,
1948.

(14) Bowen, N. L., and Tuttle, O. F.:   "The System
$MgO-SiO_2-H_2O$", Bull. G.S.A., vol. 60,
pp. 439-460, 1949.

(15) Thilo, E., and Rogge, 6:   "Chemische Untersuchungen
von Silikaten, Mitteil VIII, Ber. der Deut.
Chem. Gesell., v. 72, 341, 1939.

(16) Ahrens, L. H.: "The Spectrochemical Analysis of
Fluorine in Phosphate Rock", J. S. Afr.
Chem. Inst., vol. 25, 18, 1942.

(17) Kelley, K. K.: "The Entropies of Inorganic Substances",
Bur. of Mines Bull., No. 350, p. 48, 1932.

(18) --------- Unpublished Data, Dept. of Geology, M.I.T.,
1951.

(19) Roberts, E.C.: Unpublished Thesis, Dept. of Met.,
M.I.T., 1951.

(20) Winchell, A. N., and Winchell, H.: Elements of
Optical Mineralogy, John Wiley and Sons,
N. Y., 1951.

(21) Comeforo, J. E., Hatch, R. A., and Eitel, W.:
"Isomorphism of Synthetic Fluorine -
Amphiboles", Program 1950 Annual Meetings,
Geological Society of America.

(22) Buerger, M. J.: "The Role of Temperature in Mineralogy",
Am. Min., vol. 33, pp. 101-121, 1948.

(23) Berg, M.:   Unpublished Thesis, Dept. of Met., M.I.T.,
1951.

(24) White, W. P.: "Silicate Specific Heats, Second Series",
Am. J. Sci., vol. 47, pp. 1-43, 1919.

(37) Strunz, H.:   <u>Minerallen Tabellen</u>, Leipzig, 1941.

(38) Becker, K.:   "Eine Röentgenographische Methode zur
                   Bestimmung des Wärmeausdehnungskoeffi-
                   zienten bei Hohen Temperaturen",
                   <u>Z. Physik</u>, vol. 40, 37, 1926-7.

(39) Wells, A.F.: <u>Structural Inorganic Chemistry</u>, Oxford
                   Univ. Press, 1945.

(40) Sundius, N.: "The Position of Richterite in the
                   Amphibole Group", <u>Geol. För. För.</u>,
                   Band 67, pp. 266-270, 1945.

(41) Sundius, N.: "The Optical Properties of Manganese-
                   Poor Grunerits and Cummingtonites,
                   Compared with those of Manganiferous
                   Members", <u>Am. J. Sci.</u>, vol. 22, pp. 340-
                   344, 1931.

(42) Sundius, N.: "Die Chemische Zusammensetzung des
                   Holmquistits", <u>Geol. For. För.</u>, Band 69,
                   pp. 51-54, 1947.

(43) Larson, E. S.: "Alkalic Rocks of Iron Hill, Gunnison
                   County, Colorado", <u>U.S.G.S.P.P.</u> 197A,
                   1942.

(25) Rankama, K., and Sahama, Th. G: Geochemistry, The University of Chicago Press, 1949.

(26) Landergren, S.: "On the Geochemistry of Swedish Iron Ore and Associated Rocks", Sver. Geol. Unders., Ser. C. No. 496, Årsbok 42, no. 5, 1948.

(27) Lundegårdh, P. H.: "Rock Composition and Development in Central Roslagen, Sweden", Arkiv Kemi, Min. Geol., 23A, 9, 1946.

(28) Doelter, C., and Hussak, E.: Neues Jahrbuch, 1, 18, 1884.

(29) Des Cloizeaux, A.: Doelter's Handbuch der Mineralogie, S. 633, Bard II, Erste Halefte.

(30) Belowski, M.: Neues Jahrbuch für Mineralogie, Bd. I, p. 219, 1891.

(31) Weinschenk, E.: Petrographic Methods, pp. 291-292, 1912.

(32) Kôzu, S., Yoshiki, B., and Kani, K.: "Note on the Study of the transformation of Common Hornblende into Basaltic Hornblende at 750°C.", Sci. Rept. Tokoku Imp. Univ., Ser. 3., vol. 3, No. 2, p. 143, 1927.

(33) Barnes, V.E.: "Changes in Hornblende at about 800°C. Am. Min., vol. 15, p. 393-417, 1930.

(34) Warren, B. E.: "The Crystal Structure and Chemical Composition of the Monoclinic Amphiboles", Zeit. fur Krist., vol. 72, pp. 493-517, 1930.

(35) Sundius, N.: "The Classification of the Hornblendes and the Solid Solution Relations in the Amphibole Group", Sver. Geol. Unders., Ser. C. No. 480, Årsbok 40, No. 4, pp. 1-36, 1946.

(36) Shinoda, G.: "X-ray Investigations on the Thermal Expansion of Solids", Mem. Coll. of Sci., Kyoto Imp. Univ., Ser. A., 16, 193, 1933.

Biographical Note

Mark Caesar Wittels, son of Mr. and Mrs. I. L. Wittels of Minneapolis, Minnesota, was born in that city on July 14, 1921. Having attended the public schools in Minneapolis, he graduated from South High School in 1939. His undergraduate college training was completed at the University of Minnesota in August, 1947, where he received a B.S. degree. During the years 1941-1945 his undergraduate training was interrupted while he served in the Air Forces of the U. S. Army.

In September, 1947, he entered the M.I.T. Graduate School as a research assistant in Geology, which position he held for one year. The research was mainly concerned with experimental rock deformation. During the school year 1948-1949 he was a teaching fellow in Geology and assisted in the mineralogy course. He was made an associate member of Sigma Xi in 1950.